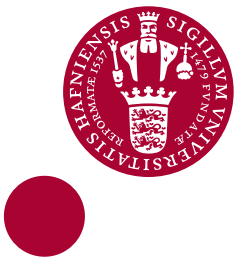

Mid-Miocene record of large-scale Snake River- type explosive volcanism and associated subsidence on the Yellowstone hotspot track

the Cassia Formation of Idaho, USA

Knott, Thomas R.; Branney, Michael J.; Reichow, Marc K.; Finn, David R.; Coe, Robert S.; Storey, Michael; Barfod, Dan; McCurry, Michael

Published in:
Geological Society of America Bulletin

DOI:
10.1130/B31324.1

Publication date:
2016

Document version
Publisher's PDF, also known as Version of record

Mid-Miocene record of large-scale Snake River–type explosive volcanism and associated subsidence on the Yellowstone hotspot track: The Cassia Formation of Idaho, USA

Thomas R. Knott[1,†], Michael J. Branney[1], Marc K. Reichow[1], David R. Finn[2], Robert S. Coe[2], Michael Storey[3], Dan Barfod[4], and Michael McCurry[5]

[1]*Department of Geology, University of Leicester, Leicester, LE1 7RH, UK*
[2]*Earth and Planetary Science Department, University of California, Santa Cruz, California 95064, USA*
[3]*Quaternary Dating Laboratory, Natural History Museum of Denmark, University of Copenhagen, 2100 Copenhagen, Denmark*
[4]*Scottish Universities Environmental Research Centre, East Kilbride, G75 0QF, UK*
[5]*Department of Geosciences, Idaho State University, Pocatello, Idaho 83209, USA*

ABSTRACT

The 1.95-km-thick Cassia Formation, defined in the Cassia Hills at the southern margin of the Snake River Plain, Idaho, consists of 12 refined and newly described rhyolitic members, each with distinctive field, geochemical, mineralogical, geochronological, and paleomagnetic characteristics. It records voluminous high-temperature, Snake River–type explosive eruptions between ca. 11.3 Ma and ca. 8.1 Ma that emplaced intensely welded rheomorphic ignimbrites and associated ash-fall layers. One ignimbrite records the ca. 8.1 Ma Castleford Crossing eruption, which was of supereruption magnitude (~1900 km^3). It covers 14,000 km^2 and exceeds 1.35 km thickness within a subsided, proximal caldera-like depocenter. Major- and trace-element data define three successive temporal trends toward less-evolved rhyolitic compositions, separated by abrupt returns to more-evolved compositions. These cycles are thought to reflect increasing mantle-derived basaltic intraplating and hybridization of a midcrustal region, coupled with shallower fractionation in upper-crustal magma reservoirs. The onset of each new cycle is thought to record renewed intraplating at an adjacent region of crust, possibly as the North American plate migrated westward over the Yellowstone hotspot. A regional NE-trending monocline, here termed the Cassia monocline, was formed by synvolcanic deformation and subsidence of the intracontinental Snake River basin. Its structural and topographic evolution is reconstructed using thickness variations, offlap relations, and rheomorphic transport indicators in the successive dated ignimbrites. The subsidence is thought to have occurred in response to incremental loading and modification of the crust by the mantle-derived basaltic magmas. During this time, the area also underwent NW-trending faulting related to opening of the western Snake River rift and E-W Basin and Range extension. The large eruptions probably had different source locations, all within the subsiding basin. The proximal Miocene topography was thus in marked contrast to the more elevated present-day Yellowstone plateau.

INTRODUCTION

The Yellowstone–Snake River Plain volcanic province, United States (Fig. 1), is the youngest and best-preserved silicic intraplate volcanic province on Earth, with a protracted history of voluminous explosive eruptions from the mid-Miocene to the present (e.g., Pierce and Morgan, 1992; Bonnichsen et al., 2008). It produced the largest known volume of low $\delta^{18}O$ deposits on Earth (e.g., Boroughs et al., 2005) and is the type locality of high-temperature "Snake-River–type" supereruptions, which generated vast, intensely welded, and commonly lava-like rheomorphic ignimbrites, thick laminated ash-fall deposits, and uncommonly long block lavas (Branney et al., 2008). Of great interest is the unusual physical volcanology of these large eruptions, and the ways in which the magmas formed and varied with time as the continental hotspot migrated eastward (Fig. 1; Leeman et al., 2008; Shervais et al., 2013). Some of the eruptions are predicted to have been as large as the better-known eruptions from Yellowstone (Ellis et al., 2012), yet large tracts of the province remain little studied, and the overall volcanic stratigraphy is not resolved. Pioneering work by Bonnichsen et al. (2008) summarized known rhyolitic volcanic units around the central Snake River Plain, but an essential step toward understanding the magmatic and structural evolution of the province through time will be to develop a stratigraphic and chronologic framework of sufficient resolution to permit the robust distinction and characterization of the individual eruptions.

This paper documents the 1.95-km-thick volcanic succession around the Cassia Hills on the southern flank of the central Snake River Plain, Idaho (Fig. 1), where deep canyon incision, together with a new 1.9-km-deep borehole, reveal one of the most complete successions of mid-Miocene Snake River volcanism in the region. The study builds on previous work (Williams et al., 1990; Wright et al., 2002; Ellis et al., 2010) and resolves earlier groupings and miscorrelations of eruption units. We present new stratigraphic definitions, and we characterize 12 major rhyolitic explosive eruptions that occurred between 11.3 Ma and ca. 8 Ma, during a major ignimbrite flare-up within the province (Nash et al., 2006) broadly contemporaneous with the opening of the western Snake River continental rift (Bonnichsen et al., 2008; Fig. 1). Where possible, unit names are retained from earlier accounts. New field descriptions, whole-rock and mineral chemistry, geochronology, and paleomagnetic data are presented to characterize and distinguish each eruption unit, and the resultant stratigraphic framework is used to reveal repeated magmatic cycles in Snake River Plain magmas over time. Finally, the tectonic and magmatic evolution of the region during the catastrophic eruptions is reconstructed from structural and deposit thickness data.

[†]trk2@le.ac.uk

GSA Bulletin; July/August 2016; v. 128; no. 7/8; p. 1121–1146; doi: 10.1130/B31324.1; 19 figures; 1 table; Data Repository item 2016049; published online 10 February 2016.

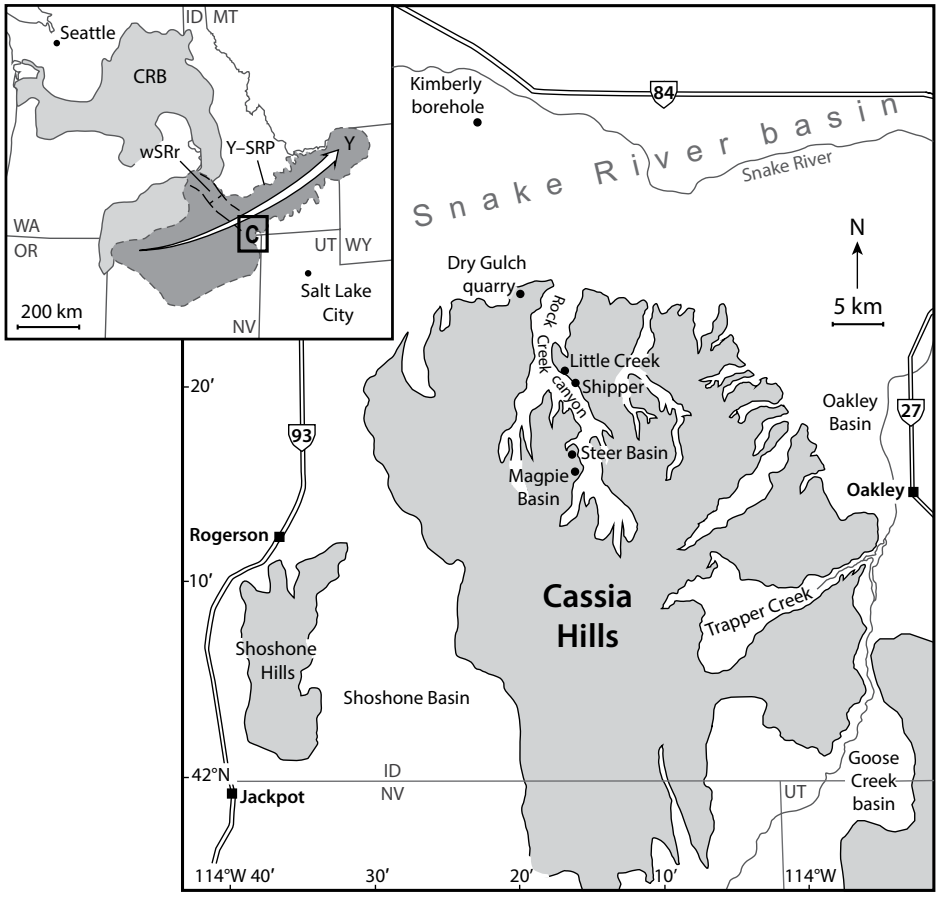

Figure 1. Map of the Cassia Hills in southern Idaho (C in inset) showing main canyons and locations mentioned in the text. Gray—elevated terrain (main map); CRB—Columbia River basalts; Y-SRP—Yellowstone–Snake River Plain volcanic province showing NE migration of the Yellowstone hotspot track (white arrow); Y—Yellowstone; wSRr—western Snake River rift. State abbreviations in inset: ID—Idaho; MT—Montana; NV—Nevada; UT—Utah; WY—Wyoming; WA—Washington; OR—Oregon.

Geological Setting

Voluminous rhyolitic volcanism associated with the Yellowstone hotspot has migrated ~600 km eastward from northern Nevada across southern Idaho, to the present-day Yellowstone volcanic field (Leeman, 1982; Pierce and Morgan, 1992). It covers ~175,000 km^2 and is commonly attributed to a mantle plume beneath the westerly migrating North American plate (Armstrong et al., 1975; Cathey and Nash, 2004; Pierce and Morgan, 1992), although slab breakoff (James et al., 2011) and crustal extension due to upper-mantle convection (Christiansen et al., 2002) also have been proposed. The rhyolites likely exceed 30,000 km^3 and are thought to have been generated by melting associated with the incremental emplacement of a large midcrustal mafic sill at a depth of ~12 km beneath the ENE-trending Snake River basin (Fig. 1; Rodgers et al., 2002; Leeman et al., 2008). This regional intracontinental basin crosses N-trending Basin and Range structures and has undergone E-W extension (Miller et al., 1999). Several vast ignimbrite sheets are exposed in massifs along the north and south flanks of the Snake River basin, and are thought to derive from various rhyolitic eruptive centers concealed beneath Neogene basalt lavas within the Snake River basin (Bonnichsen et al., 2008). Associated tephras are dispersed widely across the continental United States (Perkins et al., 1998).

The Cassia range in southern Idaho and northern Nevada has a relief of ~1100 m and is bounded by the Snake River, Oakley, Goose Creek, and Shoshone basins (Fig. 1). It is intensely faulted, and deep valleys (e.g., Rock Creek Canyon; Fig. 1) expose late Paleozoic basement unconformably overlain by mid-Miocene volcanic strata. The basement consists of mid-Ordovician marine limestone and orthoquartzite in the west, and more widespread Lower Permian sandstones and limestone (Youngquist and Haegele, 1956; Mytton et al., 1990; Williams et al., 1991). The cover is composed of intensely welded Snake River–type rhyolitic ignimbrites and associated ashfall deposits (Branney et al., 2008), inferred to have originated from the central Snake River Plain (Pierce and Morgan, 1992; McCurry et al., 1996).

Methods

Successions in canyon walls were subdivided into eruption units (deposit packages inferred to record a single volcanic eruption) on the basis of intervening paleosols, sedimentary horizons, and contrasting paleomagnetic signatures that indicate significant repose periods. Challenges were presented by (1) the monotonous nature of the thick ignimbrite successions and (2) abundant high-angle faults that repeat units along canyon walls. Therefore, we targeted nonfaulted reference sections (and one borehole) where numerous units are exposed in stratigraphic continuity. Links between these reference sections were then resolved by detailed mapping to elucidate lateral lithological and thickness variations. Lithostratigraphic units (members) are defined at type sections (coordinates in Table S1[1]). More than 30 logs were described, and tops and bases of units were sampled (Table S1 [see footnote 1]) for petrographic, geochemical, radioisotopic, and paleomagnetic analysis. Fresh vitrophyres with negligible accidental material were selected for whole-rock major- and trace-element X-ray fluorescence (XRF) analysis. Mineral phases were characterized in thin section and by electron microprobe analyses. For consistency, all paleomagnetic samples were drilled at the same sites as the geochemical sampling, and were analyzed following methods outlined in Finn et al. (2015). Individual members were dated variously by single-crystal $^{40}Ar/^{39}Ar$ dating of feldspars and U-Pb dating of zircons, and we present new data alongside published ages in Table 1. Analytical procedures, data, sample locations, standards, and applied corrections are given in the GSA Data Repository (see footnote 1).

CASSIA FORMATION

The mid-Miocene Cassia Formation of the Cassia Hills is part of the Idavada Volcanic Group (Malde and Powers, 1962; Ellis et al., 2010). It rests upon Paleozoic–Mesozoic base-

[1]GSA Data Repository item 2016049, analytical methods and data interpretations, Figures S1 and S2, and Tables S1–S6, is available at http://www.geosociety.org/pubs/ft2016.htm or by request to editing@geosociety.org.

TABLE 1. SUMMARY OF RADIOISOTOPIC DATES FOR MEMBERS OF THE CASSIA FORMATION WITH SAMPLE LOCATIONS, MATERIAL TYPE, AND METHOD USED

Member	Sample number	Sample location	Sample type	Method	Weighted mean age (Ma)
Shoshone Rhyolite	A2 751.6-754	Kimberly borehole	Plagioclase	Single-grain laser fusion	6.37 ± 0.44*
Kimberly Member	A2 1419-1424	Kimberly borehole	Sanidine	Single-grain laser fusion	8.109 ± 0.046*
	A2 1945-1953	Kimberly borehole	Sanidine	Single-grain laser fusion	7.951 ± 0.110*
Castleford Crossing Member	A2 2102-2106	Kimberly borehole	Plagioclase	Single-grain laser fusion	7.93 ± 0.48*
	MBH-12.2-013	E-Bennett Mts	Plagioclase	Single-grain laser fusion	8.10 ± 0.42*
	–	Cotterel Hills	Zircon	Ion microprobe (SHRIMP-RG)	8.19 ± 0.19#
Lincoln Reservoir Member	RC-10.1-008	Little Creek section	Plagioclase	Single-grain laser fusion	8.69 ± 0.90*
	TC-12.1-012	Trapper Creek	Plagioclase	Single-grain laser fusion	7.97 ± 0.30*
McMullen Creek Member	RC-10.1-006	Little Creek section	Zircon	Ion microprobe (SIMS)	9.0 ± 0.2*
Indian Springs Member	RC-10.1-010	Little Creek section	Zircon	Ion microprobe (SIMS)	9.0 ± 0.3*
Dry Gulch Member	DG-11.1-004	Dry Gulch	Plagioclase	Single-grain laser fusion	8.63 ± 0.50*
	Q2-11.1-001	~4 km west of Dry Gulch	Plagioclase	Single-grain laser fusion	8.47 ± 0.19*
Little Creek Member	RC-11.1-004	Little Creek section	Zircon	Ion microprobe (SIMS)	10.3 ± 0.2*
Wooden Shoe Member	RC-10.1-002	Little Creek section	Sanidine	Single-grain laser fusion	10.139 ± 0.006*
	–	Trapper Creek	Sanidine	Multigrain laser fusion	10.25 ± 0.06§
Steer Basin Member	–	Rock Creek	Sanidine + plagioclase	Single-grain laser fusion	10.62 ± 0.09†
Big Bluff Member	RC-10.1-011	Magpie Basin	Sanidine	Single- grain laser fusion	10.952 ± 0.010*
		Magpie Basin	Sanidine + plagioclase	Single-grain laser fusion	10.97 ± 0.07†
		Trapper Creek	Sanidine	Multigrain laser fusion	11.05 ± 0.03§
Magpie Basin Member	MP-11.2-001	Magpie Basin	Sanidine	Single-grain laser fusion	11.337 ± 0.008*

Note: All argon ages are relative to feldspar Fish Canyon sanidine (FCs) standard at 28.172 Ma ± 0.028 Ma (Rivera et al., 2011) and are reported with 2σ uncertainties. SHRIMP-RG—sensitive high-resolution ion microprobe–reverse geometry; SIMS—secondary ion mass spectrometry.

*This study (see supplementary Tables S3 and S4; see text footnote 1).

†Ellis et al. (2012).

§Perkins et al. (1995).

#Konstantinou et al. (2012).

ment, and locally on Miocene volcaniclastic sediments (formerly "Tuff of Ibex Peak"; Mytton et al., 1990). Within the Snake River basin, it is overlain by the ca. 6 Ma Shoshone Rhyolite lava and younger volcaniclastic sediments and basalt lavas (Bonnichsen and Godchaux, 2002). The formation consists of 12 members, and each member is interpreted as a rhyolitic eruption unit (Fig. 2). The two uppermost members are seen in the 1.9-km-deep Kimberly borehole, just north of the Cassia Hills (Fig. 1). The base of the Cassia Formation is defined as the base of the welded Magpie Basin Member (the lowest eruption unit), and its top is defined at the upper contact of the Kimberly Member as seen in the Kimberly borehole.

Earlier regional mapping (Mytton et al., 1990; Williams et al., 1990, 1991, 1999) distinguished five welded volcanic units separated by three nonwelded units, some of which were further subdivided (e.g., "Tuff of McMullen Creek" members 1–5 of Wright et al., 2002). The present study defines each member at type localities in four principal reference sections: Little Creek and Magpie Basin sections in Rock Creek Canyon, Dry Gulch quarry on the north slopes, and the Kimberly borehole in the southern Snake River Plain (Fig. 1). For quick reference, a summary of the distinguishing characteristics of each member is given in the data repository (Table S6; see footnote 1).

Magpie Basin Member

The Magpie Basin Member ("Tuff of Magpie Basin" of Williams et al., 1991; Ellis et al., 2010) is an intensely welded ignimbrite with a basal ash-fall layer. It is the oldest member of the Cassia Formation and is defined at its type locality, Magpie Basin (Fig. 1), where it unconformably overlies an irregular paleotopography on the Permian limestone basement and is overlapped by the Big Bluff Member. The ignimbrite is a high-silica rhyolite (~75 wt% SiO_2) with low TiO_2 (0.3–0.4 wt%), CaO (0.7–0.8 wt%), and Ba (<1000 ppm), and it is chemically similar to the overlying Big Bluff Member. It can, however, be distinguished from other members of the formation by having a reversed magnetic polarity (Fig. 3) and lower phenocryst content (~5%). The member varies in thickness abruptly from 30 m thick in paleovalleys to less than 10 m on paleotopographic highs. We provide a sanidine $^{40}Ar/^{39}Ar$ date of 11.337 ± 0.008 Ma (Table 1).

A white, parallel-bedded, fine ash-fall layer, 5 m thick, contains a few beds of angular pumice clasts 3–5 mm in size, and darkens upward due to incipient fusing by the overlying welded ignimbrite. The ignimbrite is a simple cooling unit (sensu Smith, 1960), ≤25 m thick, with lower and upper vitrophyric zones that enclose a thick central lithoidal zone with sheet joints (Fig. 4A). Where the ignimbrite thins to less than 10 m, the central lithoidal zone pinches out and is marked only by a central zone of lithophysae and axiolites (Fig. 4). Rheomorphic attenuation of shards and microscopic intrafolial isoclinal folding of the subhorizontal eutaxitic foliation occur in the basal vitrophyre, but, unlike many of the overlying members, macroscopic folding is limited. Welding and rheomorphism decrease with height, and the upper vitrophyre contains weakly welded shards with bi- and tricuspate shapes. The ignimbrite is composed of lithic-poor massive tuff and is probably a single flow unit with no time gaps recorded during its emplacement. It contains sanidine, plagioclase, augite, pigeonite, ilmenite, magnetite, rare quartz, and accessory zircon and apatite—a common assemblage for Snake River Plain ignimbrites (Wright et al., 2002; Bonnichsen et al., 2008; Ellis et al., 2013). The phenocrysts (1–4 mm) occur as discrete crystals and in polycrystalline aggregates of two pyroxenes, feldspar, and Fe-Ti oxides, or as aggregates without feldspar; similar features are reported from units elsewhere in the province (Cathey and Nash, 2004; Ellis et al., 2014).

Big Bluff Member

The Big Bluff Member (Ellis et al., 2010; "Tuff of Big Bluff" of Williams et al., 1990) is the thickest member of the Cassia Formation,

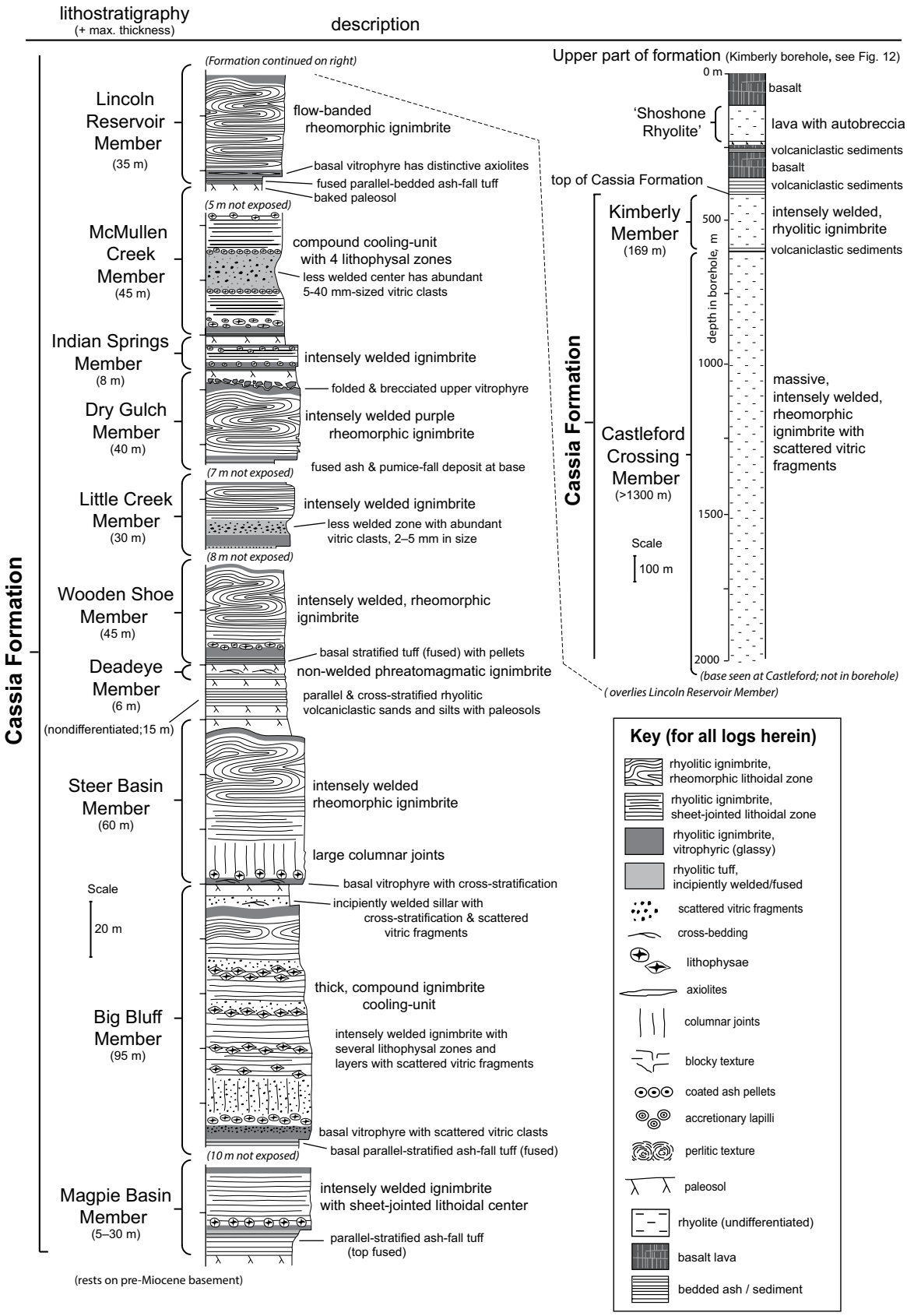

Figure 2. Generalized vertical stratigraphy of the Cassia Formation in southern Idaho. Note smaller vertical scale of upper section (right).

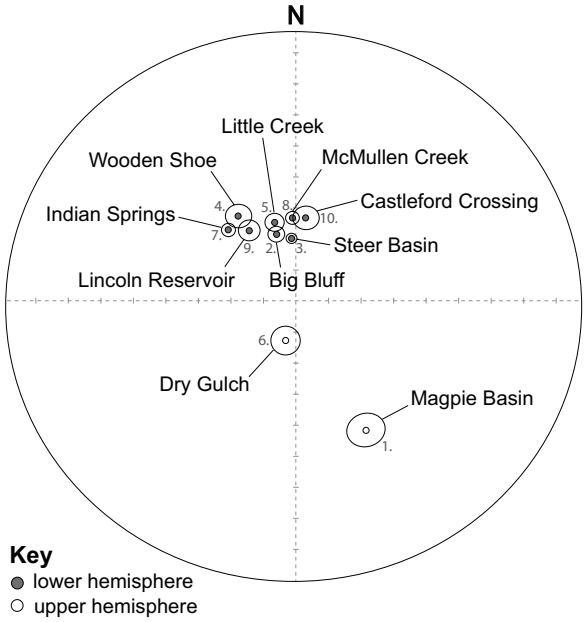

Figure 3. Geographic stereonet showing the site mean paleomagnetic (thermoremanent magnetization) directions of Cassia Formation members (n = ≥10 per site) not corrected for tectonic dips. Note that the mean direction of each member is clearly distinct from that of immediately enclosing units. Members numbered from 1 (oldest) to 10 (youngest) to clarify relative stratigraphic positions.

with a new sanidine $^{40}Ar/^{39}Ar$ age of 10.952 ± 0.010 Ma (Table 1). It is defined at a type locality in Magpie Basin (Fig. 1), where it overlaps the Magpie Basin Member to rest unconformably on irregular Permian basement. It is overlain locally by undifferentiated white, parallel- and cross-stratified volcaniclastic sands, 25 m thick (Tt1 of Williams et al., 1991), and by the Steer Basin Member.

A basal ash-fall layer, ≥2 m thick, is overlain by a welded ignimbrite, ~95 m thick (Fig. 5). The ash-fall layer is parallel bedded and has been fused to vitrophyre by the ignimbrite (Fig. 5). The welded ignimbrite is composed of lava-like, massive to flow-laminated tuff and lapilli-tuff. Lithophysal zones correspond with present-day erosional benches (Fig. 5D). Although lithic lapilli are rare, blocky, nonvesicular vitric fragments (<20 mm in size; Fig. 5C) occur in the lower vitrophyre, the lower lithoidal zone, and in 2-m-thick layers higher in the lithoidal zone. Platy joints become more prominent with height, and meter-scale open rheomorphic folds are common in the upper 10 m. Above the folded upper vitrophyre, a 5-m-thick pink sillar (lapilli-tuff indurated by vapor-phase cement) contains abundant matrix-supported, blocky vitric lapilli, and local diffuse low-angle cross-bedding. The sillar is hardly welded, but its lowermost few centimeters have been locally back-fused at the contact with the formerly hot, underlying vitrophyre. The top of the member has an orange paleosol.

The Big Bluff Member is a high-silica rhyolite (SiO_2 ~75 wt%) with 2%–15% crystals, 1–4 mm in size. Its mineral assemblage consists of sanidine, plagioclase, augite, magnetite, ilmenite, and accessory apatite and zircon, all of which are common to most Snake River ignimbrites. However, it can be distinguished from the other members by the presence of fayalitic olivine, abundant quartz, and an absence of pigeonite (which is present in all other members; Fig. 6). It also has a lower barium content (<1000 ppm) and higher Rb/Sr ratios (Rb/Sr >4) compared to the overlying members (Table S1; see footnote 1).

Interpretation

Initial ash fall from a tall eruption column was followed by emplacement of a widespread and prolonged, very hot (above the glass transition) pyroclastic density current that deposited the thick, rheomorphic ignimbrite. Successive quenching events during aggradation of the compound ignimbrite cooling unit (sensu Smith, 1960) are recorded by the lithophysal zones within the thick lithoidal zone. Each of the relatively rapidly cooled horizons may record a cooling break between successive hot pyroclastic density currents. However, several of the lithophysal zones bound layers that are rich in nonvesicular

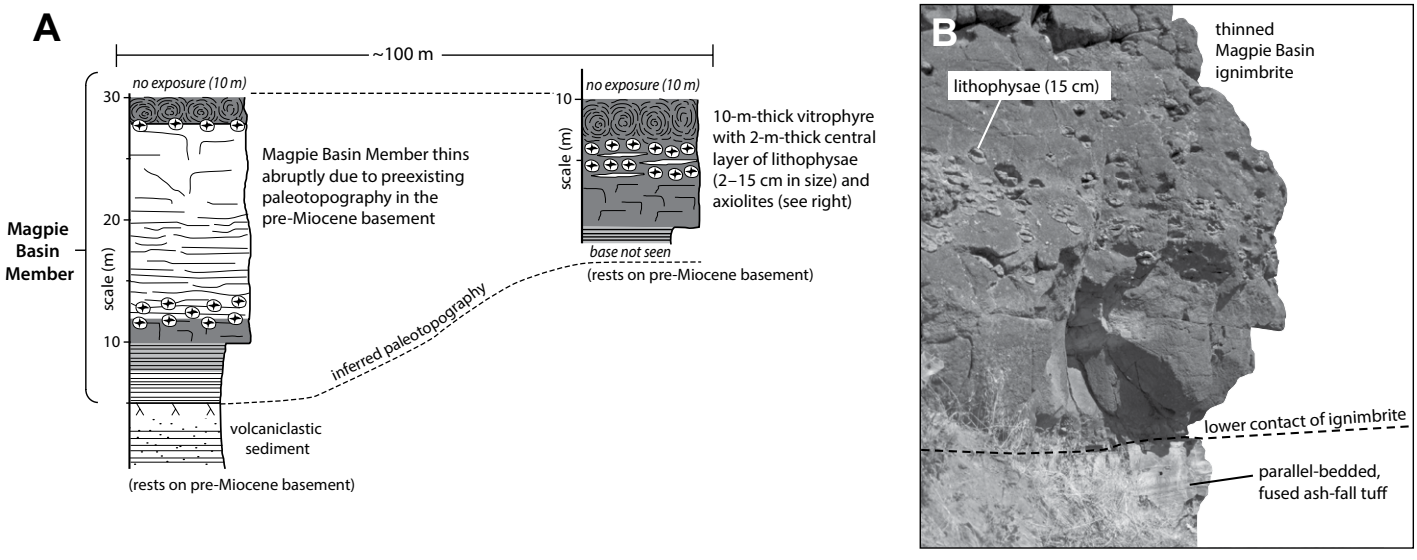

Figure 4. (A) Lateral thickness and facies variations of the Magpie Basin Member resulting from the underlying basement paleotopography, best seen at Magpie Basin (42°15′01.7″N, 114°15′49.2″W). (B) The thin, vitrophyric Magpie Basin Member showing the central zone of abundant spherulites and lithophysae.

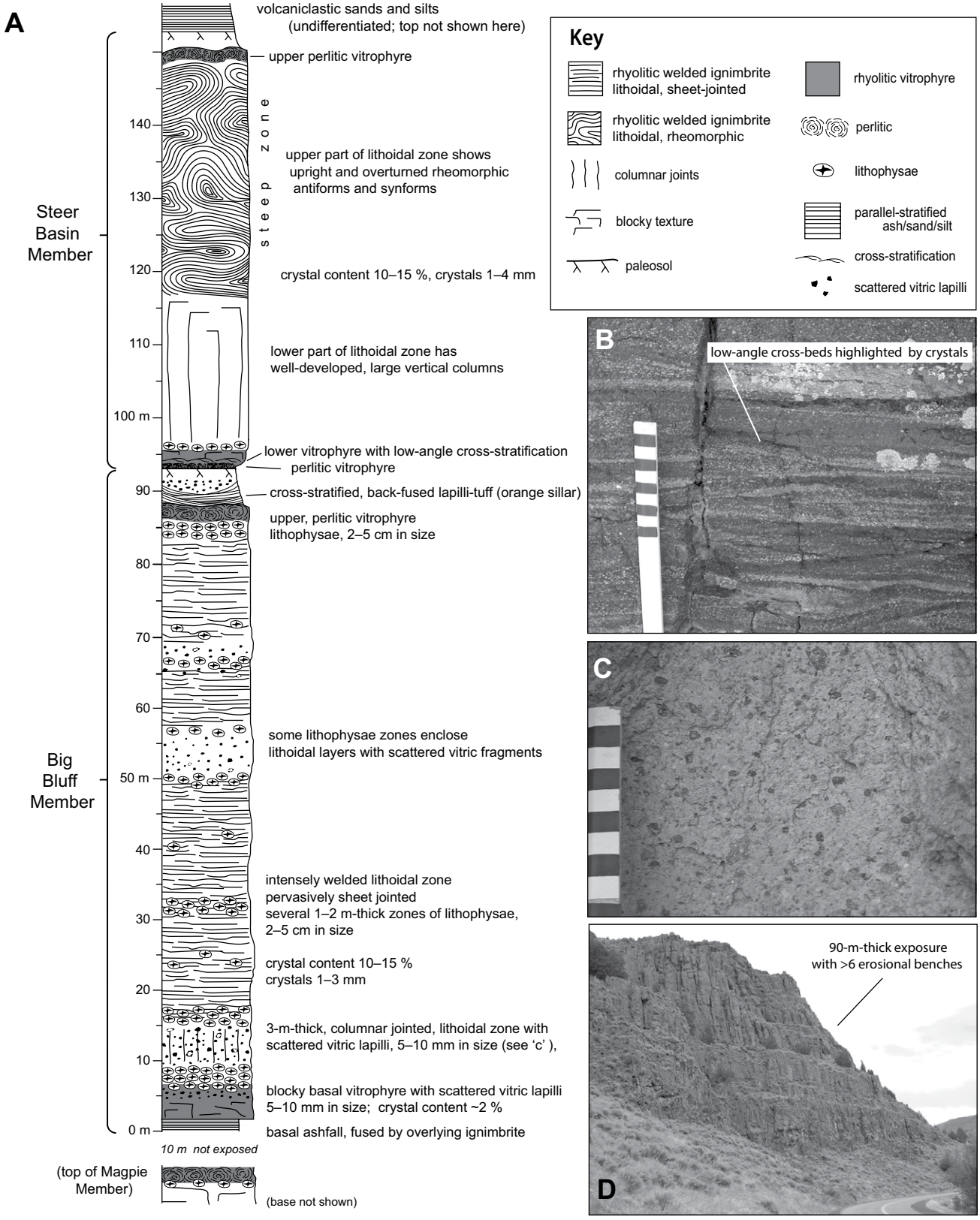

Figure 5. (A) Big Bluff and Steer Basin Members, at Magpie Basin (42°15′01.3″N, 114°15′51.2″W). (B) Low-angle cross-stratification highlighted by crystals in the lower vitrophyre of the Steer Basin Member. (C) Abundant scattered angular vitric fragments supported in tuff matrix in the lower lithoidal zone of the Big Bluff Member. (D) Big Bluff Member in Rock Creek Canyon: Benches mark successive lithophysal zones showing the compound nature of the ignimbrite.

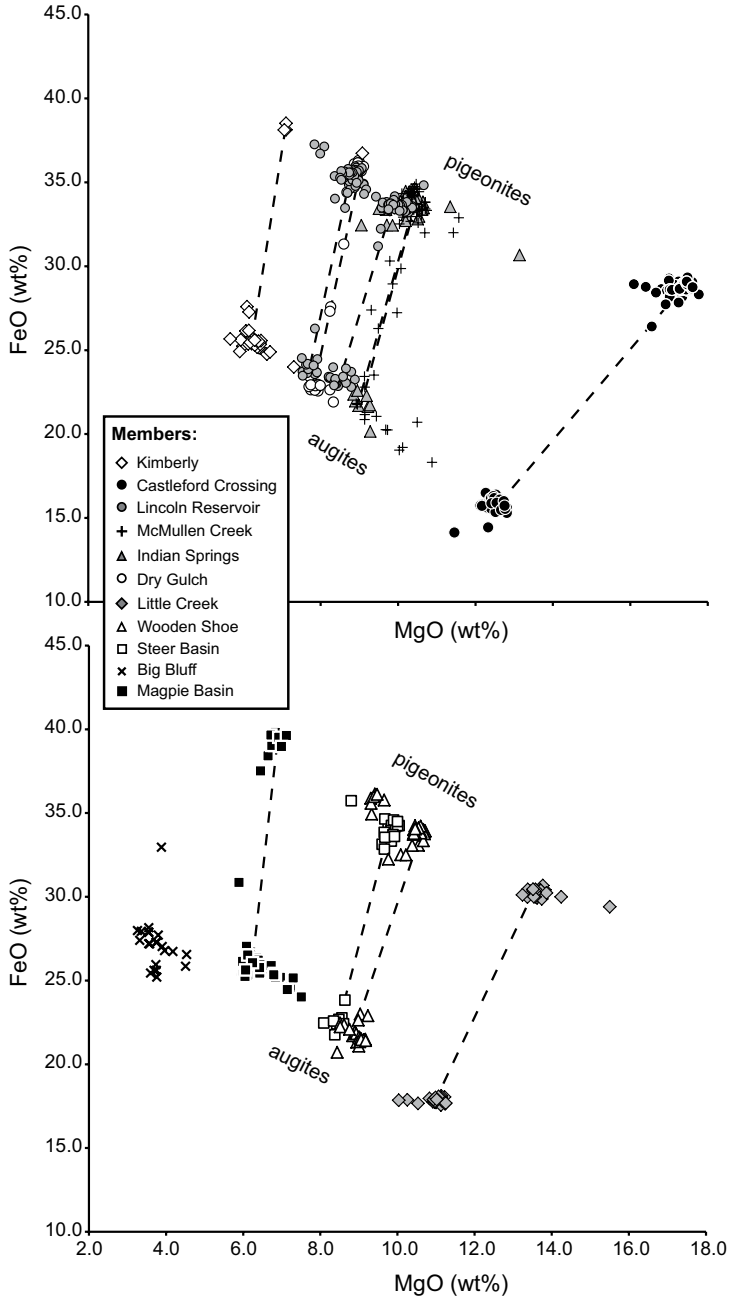

Figure 6. MgO vs. FeO plots showing the distinctive pyroxene chemistries of members of the Cassia Formation. Note that some members (e.g., Lincoln Reservoir Member) contain multiple distinct populations of pigeonite and/or augite, whereas others (e.g., Little Creek Member) show single populations of pigeonite and augite, and the Big Bluff Member has augite only. Dashes indicate equilibrium pairs.

vitric lapilli: This suggests, alternatively, that a relatively prolonged density current of high temperature may have been cooled temporarily from time to time, during successive influxes of vitric lapilli. The last such cooler influx deposited the upper, nonwelded lapilli-tuff sillar (Fig. 5). Any pauses between currents must have been brief because there are no internal coignimbrite ash-fall layers or other breaks. Contact fusing at the lower contact of the sillar indicates that the last density current passed by and deposited the uppermost layer before the underlying, welded part of the ignimbrite had cooled. The intermittent phases of cooler emplacement may have been due to (1) enhanced cooling during transport, for example, during periods of fully dilute, turbulent flow (indicated by the cross-stratification in the upper pink sillar), causing increased ingestion of cool atmospheric air; or (2) periodic entrainment into the current of copious blocky vitric fragments that were already cool (i.e., nonjuvenile) and acted as heat sinks (e.g., Marti et al., 1991). Such entrainment of preexisting vitric rhyolite from the source area (e.g., conduit or crater walls) must have been rapid, and possibly facilitated by explosive interactions with groundwater or surface water during the eruption. The Big Bluff Member is also part of a large-volume (~1000 km^3), regionally extensive eruption unit correlated with the Cougar Point Tuff XIII of Ellis et al. (2012). Therefore, the volume of the vitric lapilli seems too large (several tens of cubic kilometers) to represent ejected hot agglutinate juvenile glass temporarily adhered to conduit walls (cf. Rust et al., 2004). It may be that large volumes of glassy rhyolite (i.e., hyaloclastite) were entrained from a closer source. We speculate that a voluminous glass source, possibly a sublacustrine aquifer of glassy rhyolite, underwent repeated disruption during the Big Bluff eruption. Such disruption may have been during caldera subsidence, and could have involved hydromagmatic interactions that fluctuated with time during the prolonged and largely magmatic high-temperature explosive eruption.

Steer Basin Member

The Steer Basin Member is an ~60-m-thick, intensely welded, lava-like rhyolitic ignimbrite sheet (Fig. 5) defined at its type locality in Rock Creek Canyon (Shipper section; Fig. 1). There, the member overlies a paleosol in the top of nonwelded volcaniclastic sands (Tt1 of Williams et al., 1991) and is overlain by younger volcaniclastic sediments (see following). It contains 10%–15% of 1–4 mm crystals with an assemblage common to other central Snake River Plain ignimbrites. The member is readily distinguished from surrounding rhyolitic units by (1) its stratigraphic position, (2) the presence of a 0.3-m-thick layer of perlitic obsidian at the base, (3) diffuse low-angle cross-bedding in the lower vitrophyre (Fig. 5B), (4) a single set of tall columnar cooling joints, (5) an absence of multiple internal layers/zones (e.g., in contrast to the compound Big Bluff Member), and (6) it is chemically distinct from all other member (Fig. 7).

The lower vitrophyre is 2 m thick and contains crystals and ≤5 mm vitric fragments best seen in thin section. The vitrophyre is sharply overlain by a 55-m-thick lithoidal zone with columnar cooling joints, well developed in the

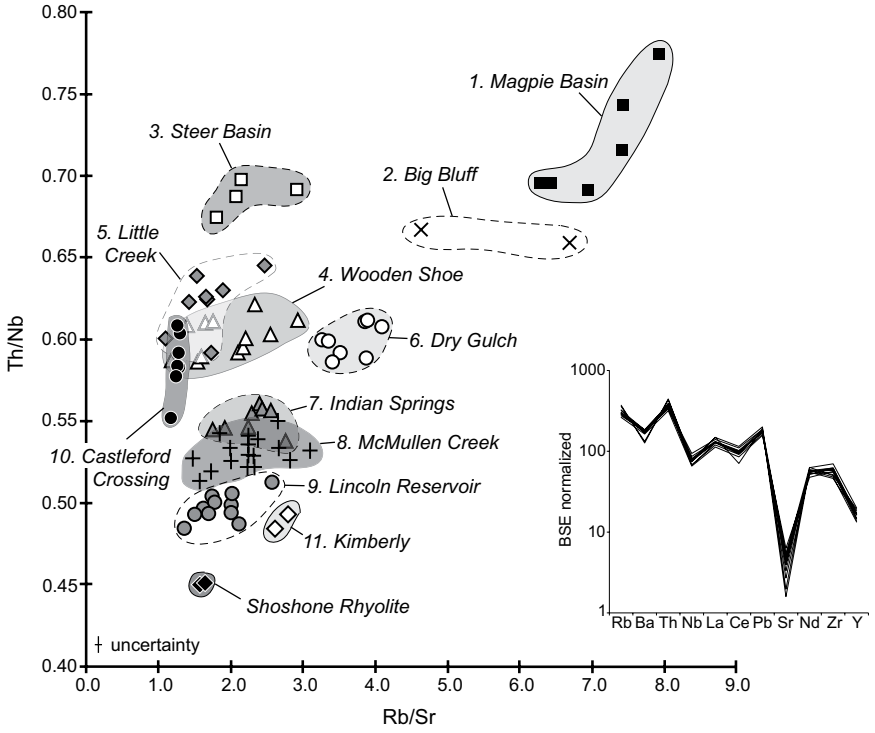

Figure 7. Rb/Sr vs. Th/Nb whole-rock data plot of the Cassia Formation. Each member forms a discrete field, although some fields overlap; where this occurs, the members are readily distinguished by intervening paleosols in the field, by discrete radioisotopic dates (Table 1), and by contrasting paleomagnetic thermoremanent magnetization directions (Fig. 3). Inset shows the bulk silicate earth (BSE)–normalized trace-element patterns for all Cassia Formation members (note: patterns are all closely similar).

lowest 20 m. Open rheomorphic folds, up to 10 m in size, occur in the top 35 m (Fig. 5A). The upper vitrophyre is 1 m thick, folded, and overlain by a pale, nonwelded, massive ash deposit preserved best within rheomorphic synclines. A weak, upper paleosol defines the top.

The member is a voluminous (~350 km^3; Ellis et al., 2012) ignimbrite sheet that extends ~80 km along the southern central Snake River Plain. It is well exposed across the Cassia Hills (Williams et al., 1990, 1991) and thins southward. In Trapper Creek (Fig. 1), it is 14 m thick, with the characteristic basal obsidian layer and overlying cross-bedding.

Interpretation

The Steer Basin Member records a single eruption, as it is a simple cooling unit without internal paleosols, fallout layers, or reworked horizons. The earliest part of the current to pass was fully dilute and turbulent (Branney and Kokelaar, 2002), indicated by the low-angle cross-bedding in the lower vitrophyre, but then it became granular fluid–based with time, as shown by the upward transition to massive tuff. The massive ash layer at the top of the member may have been deposited by a cooler density current, or as coignimbrite ash-fall subsequently disturbed by continued rheomorphic deformation in the underlying hot ignimbrite.

Volcaniclastic Sediments and Soils

About 15 m of rhyolitic volcaniclastic sand, gravel, and silt overlie the paleosol in the top of the Steer Basin Member (Fig. 2), and these are best exposed at Steer Basin (Fig. 1). A paleosol 6 m above the base was used to divide the succession into two members, the Niles Gulch and overlying Antelope Member (Ellis et al., 2010). Pumiceous gravels are overlain by thin alternations of bedded pumice sands and silts of probable fluviolacustrine origin. Above the 6 m paleosol, parallel-laminated, normal-graded sands and silts with mud-draped wave ripples are overlain by alluvial gravels, <50 cm thick, with an upper paleosol containing calcified rootlets. As the facies are predominantly sedimentary, it is not evident whether large explosive eruptions are recorded.

Deadeye Member

The Deadeye Member, 6 m thick, has been well described elsewhere (Ellis and Branney, 2010) and is defined at its type locality at Steer Basin (Fig. 1), where it overlies a paleosol in the underlying volcaniclastic sediments and is overlain by the Wooden Shoe Member. The member consists of a lower parallel-bedded ash-fall deposit, a nonwelded diffuse-stratified ignimbrite, and an upper ash-fall deposit. It is distinctively white and nonwelded with an abundance of blocky vitric fragments, ash-coated pellets, small accretionary lapilli, and irregular-shaped, variously flattened ash clumps, up to 5 cm across. A 1-m-thick orange paleosol marks the top.

Interpretation

The rhyolitic Deadeye Member was deposited at lower temperature than the other Cassia Formation members and is thought to record a phreatoplinian eruption involving proximal interaction of lake water with a hot, magmatically fragmenting pyroclastic dispersion (Ellis and Branney, 2010). The blocky vitric fragments in the ignimbrite may have a hydroclastic origin similar to those in the Big Bluff Member, but the majority of shards are cuspate and indicate the importance of magmatic exsolution during the initial explosive fragmentation.

Wooden Shoe Member

The 45-m-thick, rhyolitic Wooden Shoe Member (formerly "lower Tuff of Wooden Shoe Butte" of Williams et al., 1991) has a partly fused, thin-bedded basal ash layer overlain by a thick, intensely welded ignimbrite (Fig. 8A). We present a new high-precision sanidine $^{40}Ar/^{39}Ar$ age of 10.139 ± 0.006 Ma (Table 1). Defined at a type locality in Rock Creek Canyon (Little Creek section; Fig. 1), the member overlies the paleosol of the Deadeye Member. It is also well exposed at Steer Basin and Trapper Creek and can be distinguished from the overlying Little Creek Member by a different paleomagnetic direction (indicating a different emplacement time; Fig. 3), by mineral chemistry (Fig. 6), and by the presence of sanidine, which is absent from all overlying members.

The basal thin-bedded ash layer is 4 m thick, and its upper half is fused to vitrophyre by the welded ignimbrite. Bedding is mostly parallel but with numerous tiny scours and truncations. Horizons of abundant ash-coated pellets (≤5 mm in diameter) are a distinctive field characteristic and occur 1 m above the base, and 30 cm below the top (Fig. 8C). The basal ash layer is still 4 m thick 40 km farther south in

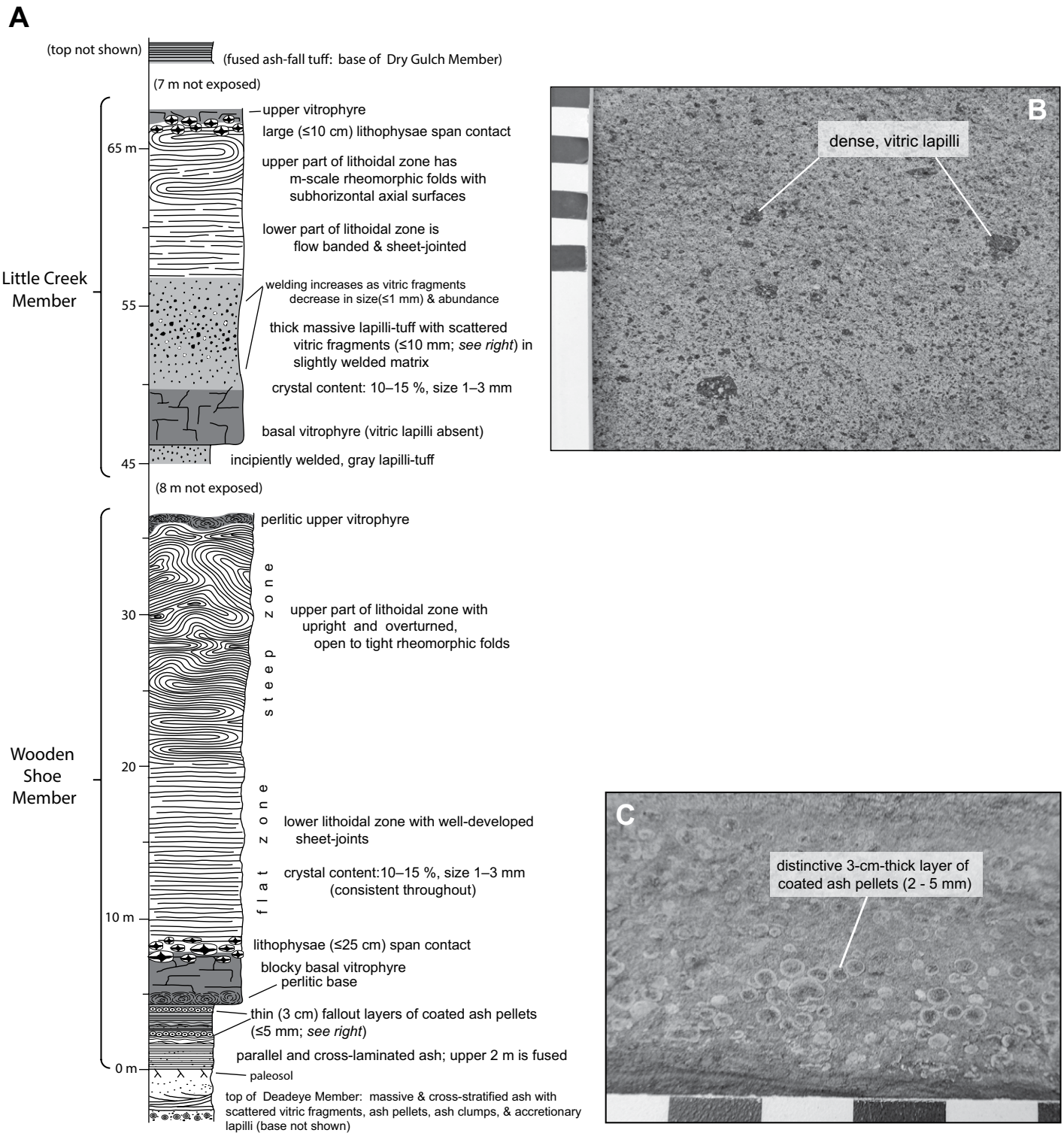

Figure 8. (A) Wooden Shoe and Little Creek Members, at Little Creek section (42°20′20.6″N, 114°17′00.0″W). (B) Abundant matrix-supported nonvesicular porphyritic vitric fragments in the central lapilli-tuff of the Little Creek Member. (C) Distinctive layer of whole and broken coated ash pellets in the stratified lower part of the Wooden Shoe Member, which includes deposits of ash-falls and fully dilute density currents.

Trapper Creek and Goose Creek basin (Fig. 1), and so it is a widespread, large-volume deposit; however, secondary thickening (reworking) precludes construction of meaningful isopachs.

The ignimbrite is lithic-poor, intensely welded massive tuff. In the south (Trapper and Goose Creeks), the base is locally erosive and nonwelded, and it has a discontinuous fines-poor vitric and crystal-rich lower layer ("ground layer" of Sparks et al., 1973). Crystals (10%–15%, 1–3 mm in size) comprise an assemblage similar to the underlying Steer Basin Member; however, the Wooden Shoe Member is the youngest in the formation to contain sanidine. The ignimbrite is a simple cooling unit with lower and upper vitrophyres and a central lithoidal zone (Fig. 8A). The lower vitrophyre is perlitic at the base and has a zone of lithophysae (≤25 cm diameter) at the top. The lithoidal zone is sheet jointed and flow banded with subhorizontal, isoclinal rheomorphic folds and pervasive sheet jointing in the lower few meters (Fig. 8A), and upright to overturned, open to tight folds near the top. A 1-m-thick upper vitrophyre overlain by a diffuse parallel-bedded gray ash is best seen at Trapper Creek (Fig. 9). The ignimbrite thins distally (southward) and in Goose Creek basin (Fig. 1) consists of a 1-m-thick perlitic vitrophyre ("Tuff of Day Canyon" of Hackett et al., 1989) overlain by cross-stratified nonwelded white ash, ~9 m thick, which passes up into an orange paleosol that marks the top of the member (Fig. 9).

Interpretation

The parallel-laminated basal ash layer is interpreted as fallout from an opening explosive phase of the Wooden Shoe eruption, but the numerous tiny scours and truncations suggest the passage of fully dilute pyroclastic density currents or localized syneruptive reworking by wind or rainwater. In addition, the ash pellet layers record moist agglomeration of ash in an atmospheric ash plume, followed by accretion of the fine ash coatings during fallout though a dusty atmosphere (as inferred in other deposits; Brown et al., 2010, 2012). These, coupled with the overall fine grain size, are consistent with subaerial fallout from a large pulsatory phreatomagmatic eruption, with a resemblance to phreatoplinian ash-fall deposits elsewhere (e.g., Branney, 1991). The ignimbrite is probably a single flow unit, and the lower "ground layer" is thought to record deposition from a more-dilute, leading part of the current, in which ash was elutriated by turbulence-induced winnowing. In the northernmost (proximal) outcrops, peperite is well developed at the base of the ignimbrite by interaction of hot welded tuff with wet substrate (Branney et al., 2008), and the basal ash-fall is unrecognizable, presumably

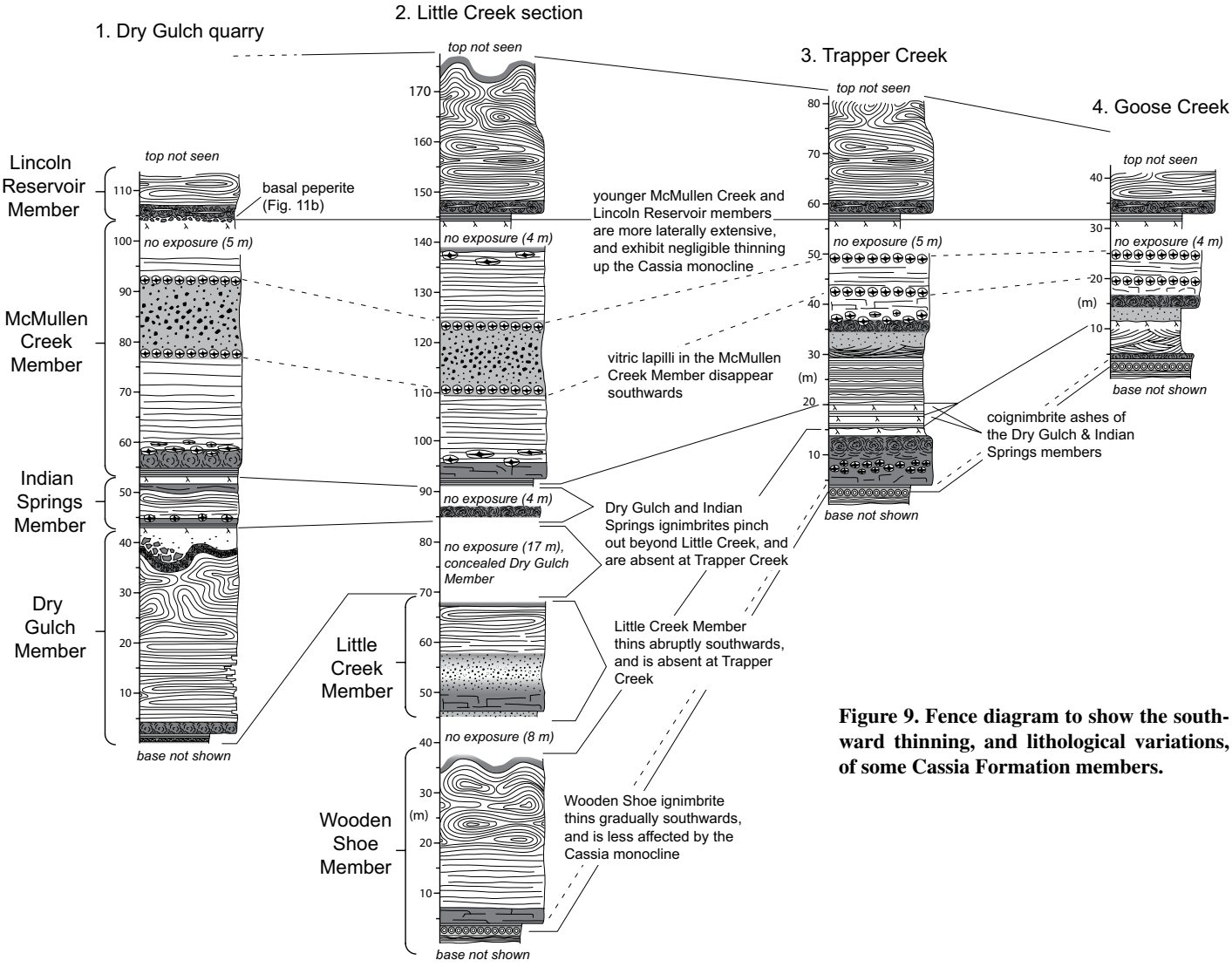

Figure 9. Fence diagram to show the southward thinning, and lithological variations, of some Cassia Formation members.

disrupted and fluidized. These relations suggest the former presence of groundwater or surface water in the southern Snake River basin at that time. The ash above the ignimbrite may be subaerial ash fall, possibly of coignimbrite origin.

Little Creek Member

The Little Creek Member (former "upper Tuff of Wooden Shoe Butte" of Williams et al., 1991; "Member 2" of Wright et al., 2002) is an ~30-m-thick rhyolitic ignimbrite with a complex welding profile: lower and upper intensely welded zones are separated by a less-welded zone with a concentration of blocky vitric fragments in a fine-tuff matrix (Fig. 8A). The member is defined at the Little Creek section (Fig. 1), where it overlies the Wooden Shoe Member and is overlain by the Dry Gulch Member (best seen ~3 km further north along Rock Creek Canyon). The ignimbrite is readily distinguishable from all others of the Cassia Formation because it contains unique high-MgO (11–14 wt%) pyroxenes (Fig. 6) and is the oldest unit in the formation without sanidine crystals.

Lowest exposures are incipiently welded, massive, gray lapilli-tuff with abundant, matrix-supported blocky vitric fragments, ≤2–5 mm. These are abruptly overlain by an intensely welded vitrophyre, 4 m thick, that lacks the blocky fragments. This, in turn, is overlain by a 6-m-thick lapilli-tuff with the return of abundant blocky vitric fragments (2–10 mm in size; Fig. 8B) that define inverse followed by normal coarse-tail grading (Fig. 8A). Welding intensity decreases toward the center, where the blocky fragments are largest, and then increases upward again toward an intensely welded massive lithoidal tuff (10 m thick), the base of which is pervasively sheet jointed. Meter-scale, subhorizontal, recumbent rheomorphic folds in the top of the unit deform the ≥1-m-thick upper vitrophyre. The Little Creek Member is restricted to the northern Cassia Hills and is absent in Trapper Creek (Fig. 9), pinching out ~2 km north of Steer Basin (Fig. 1).

Interpretation

The Little Creek Member is a compound cooling unit thought to record a single large explosive eruption, as there are no internal paleosols or reworked horizons. The lower and upper intensely welded zones indicate very hot emplacement above the glass transition, whereas the central, less intensely welded lapilli-tuff was emplaced at a slightly lower temperature. The inverse relationship between welding intensity and size and abundance of the blocky vitric fragments indicates that cooling during eruption and emplacement was associated with the incorporation of large volumes of blocky fragments. The blocky fragments may have been entrained into the pyroclastic density current in a similar manner to that inferred for the Big Bluff and Deadeye Members.

Dry Gulch Member

The rhyolitic Dry Gulch Member (former "Member 1" of Wright et al., 2002) is a layer of pumice lapilli and ash overlain by a thick rheomorphic ignimbrite (Fig. 10A). It is distinguished from all other members of the formation by its high silica content (75–76 wt%), distinct Rb/Sr and Th/Nb ratios (Fig. 7), the purple hue of its lithoidal zone, and by a distinct magnetic direction and reversed polarity, which contrasts with the normal polarity of adjacent units (Fig. 3). Dry Gulch quarry is the type locality (Fig. 1), where the member forms a single 40-m-thick eruption unit, overlain by the Indian Springs Member. The relationship with the underlying Little Creek Member is best seen in north Rock Creek Canyon.

The lowest exposure of the member is a 1.5-m-thick bedded succession that fines upward (Fig. 10D; recently concealed by spoil) and is fused by the overlying welded ignimbrite. The lower meter consists of 2–10-cm-thick beds of clast-supported angular pumice lapilli with subordinate blocky vitric fragments. The upper 0.5 m is thin-bedded medium to fine ash with low-angle cross-stratification. The ignimbrite is a simple cooling unit with lower and upper vitrophyres less than 2 m thick, and a purple flow-banded and sheet-jointed, lava-like lithoidal center. Rheomorphic folds in the lower 10 m are subhorizontal and isoclinal, but they become steeper and more open upward, with 10-m-amplitude upright to overturned anticlines and synclines in the upper 20 m. The folded upper vitrophyre is locally revesiculated to form gold-colored pumice and was faulted and autobrecciated during late-stage rheomorphism (Fig. 10C). It is overlain by nonwelded, massive and stratified ash, 3 m thick, containing 5–6-mm-sized cuspate vitric shards supported in finer ash matrix. The ash passes up into a pale-orange paleosol. Within rheomorphic synclines, the upper ash has been disturbed, oxidized and locally fused by contact with the hot ignimbrite below. The ignimbrite contains plagioclase, pigeonite, augite, magnetite, and accessory apatite and zircon, though crystals are less abundant (2%–3% and 1–3 mm in size) than in most other Cassia Formation members. Sanidine and hypersthene crystals reported by Wright et al. (2002) were not observed.

The Dry Gulch Member thins southward (distally), but it is not seen at Little Creek, where it is probably concealed beneath a 17 m slope (Fig. 9). The ignimbrite is inferred to pinch out ~6 km south of Little Creek, and it is absent further south at Trapper Creek (Fig. 1). At Trapper Creek, however, a 1.5-m-thick, nonwelded, diffuse-bedded ash deposit chemically similar to the Dry Gulch Member unconformably overlies the Wooden Shoe Member paleosol, and this may represent a distal correlative deposit, possibly of coignimbrite origin (Fig. 9).

Interpretation

The Dry Gulch Member is interpreted to record a single explosive eruption. The lower pumice and ash-fall layers record sustained subaerial fallout from an opening plinian phase. The overlying intensely welded ignimbrite was deposited from a hot pyroclastic density current that was more restricted than many Cassia Formation currents and did not travel as far south as Trapper Creek. The current was initially fully dilute, as recorded by the low-angle cross-bedding, but it soon became granular fluid–based, as recorded by the predominantly massive tuff. There is no evidence of significant time gaps during its emplacement, and the lava-like flow banding, and division into a lower flat zone and upper steep slope indicate that it was emplaced in a broadly similar manner to that inferred for the rheomorphic Grey's Landing ignimbrite (Andrews and Branney, 2011). The upper ash was deposited from cooler density currents and associated ash fallout before the ignimbrite rheomorphism had ceased, as recorded by its soft-state disruption.

Indian Springs Member

The Indian Springs Member (former "Member 3 of the Tuff of McMullen Creek" of Wright et al., 2002), is a ca. 9 Ma (Table 1), 8-m-thick rhyolitic eruption unit consisting of a basal ash fall overlain by an intensely welded ignimbrite. It is defined at Dry Gulch quarry, where it overlies the Dry Gulch Member and is overlain by the McMullen Creek Member. It has a normal paleomagnetic polarity with a paleomagnetic direction that readily distinguishes it from its enclosing members (Fig. 3).

A pale-gray, lower ash-fall layer has thin parallel bedding and is incipiently fused by the overlying welded ignimbrite (Fig. 10B). The ignimbrite has a lower perlitic vitrophyre, 1 m thick, sharply overlain by 5 m of brown massive and flow-banded lithoidal tuff. The lower 2 m section has a complex devitrification pattern with intercalated lithoidal and glassy flow bands. The upper half of the ignimbrite shows rheomorphic folds. The upper, folded vitrophyre is 2 m thick with axiolites and prolate

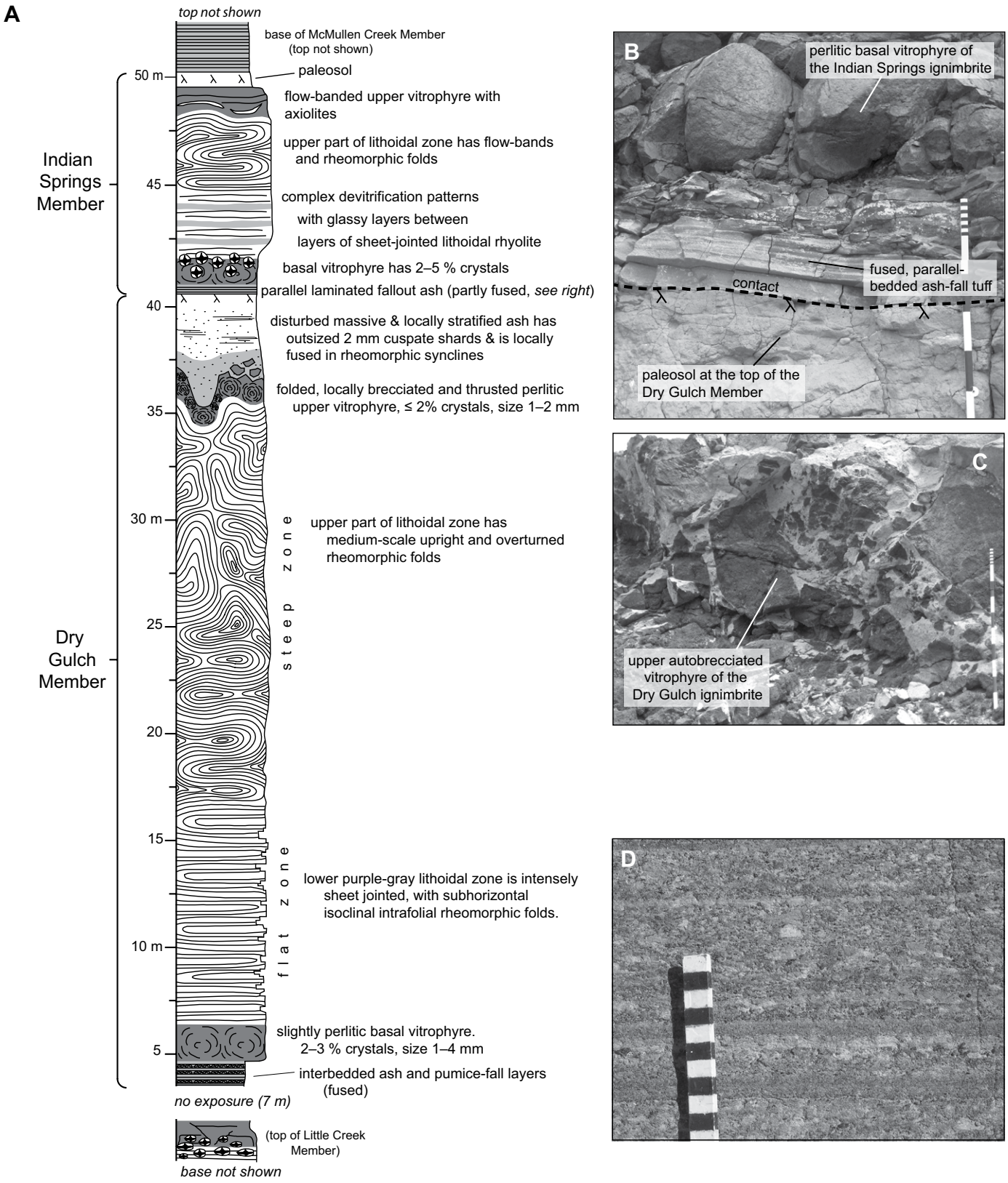

Figure 10. (A) Characteristic features of the Dry Gulch and Indian Springs Members at Dry Gulch quarry (42°24′53.0″N, 114°19′36.4″W). (B) Basal contact and lower 1 m of the Indian Springs Member. (C) Upper vitrophyric autobreccia at the top of the Dry Gulch Member with pale interstitial, percolated upper vitric (coignimbrite?) ash. (D) Parallel-bedded pumice-fall and ash-fall layers in the basal part of the Dry Gulch Member.

lithophysae along the flow banding. It is overlain by a nonwelded, parallel-bedded white ash that develops upward into a tan paleosol. The member thins southward, and the lithoidal zone pinches out so that the entire ignimbrite is vitrophyre (e.g., at the Little Creek section; Fig. 9). In Trapper Creek, a possible distal correlative parallel-bedded, nonwelded ash, 1.5 m thick, overlies the paleosol on the Dry Gulch Member (Fig. 9).

Interpretation

A single explosive eruption with no significant time gaps is inferred from the simple cooling-unit welding profile. Initial widespread subaerial ash fallout from a high eruption column was unsteady (the parallel bedding) and followed by a very high-temperature, sustained, granular fluid–based pyroclastic density current that was depletive (spatially decelerating; Kneller and Branney, 1995) as it pinches out ~2 km south of the Little Creek section. Deposition of the ignimbrite was followed by sustained fallout and deposition of the upper fine ash, possibly from a coignimbrite plume.

McMullen Creek Member

The McMullen Creek Member (locally "Goose Creek Member A" of Hackett et al., 1989; "Member 4" of Wright et al., 2002) is a rhyolitic compound ignimbrite cooling unit with a basal ash-fall layer and an upper paleosol (Fig. 11A). It is 45 m thick at its type area (Little Creek section; Fig. 1), overlies the Indian Springs Member (best seen at Dry Gulch quarry), and is overlain by the Lincoln Reservoir Member. A distinctive feature is its broad color layering when viewed from a distance: this reflects a complex vertical welding profile, with four dark vitrophyres and a central, paler lapilli-tuff (Fig. 11). We obtained a U-Pb age of 9.0 ± 0.2 Ma, which is statistically indistinguishable from the ages of the enclosing members (Table 1).

The lower ash-fall layer is 1.5 m thick, parallel laminated, and incipiently fused by the overlying ignimbrite. The ignimbrite is intensely welded, with lower and upper vitrophyres and a thick, red-brown lithoidal interior divided into two by a central, less-welded layer of lapilli-tuff, 10 m thick, with abundant matrix-supported lapilli, ≤1 cm in size, of black glassy rhyolite (Fig. 11D). Upward, the denser lapilli show inverse and then normal coarse-tail grading. The welding intensity decreases toward the center, where the lapilli are largest. The lapilli-rich layer is enclosed by dark vitrophyre zones with abundant small (≤5 cm) lithophysae. Zones of larger (≤30 cm) lithophysae span the boundaries between the lithoidal tuff and the upper and lower vitrophyres. Lapilli are absent in the upper lithoidal tuff and vitrophyre, best seen in Trapper Creek (Fig. 1), where it is overlain by orange, nonwelded massive ash. A baked orange paleosol marks the top of the member (Fig. 11C).

The member thins southward and is well exposed in Trapper Creek (30 m thick) and Goose Creek (10 m thick), where the central lapilli-tuff has pinched out, its level marked only by internal zones of lithophysae (Fig. 9). At these southern locations, the basal 1.5 m section of the ignimbrite consists of a slightly welded, low-angle, cross-bedded lapilli-tuff with small (1–5 mm) vitric lapilli. This distal facies of the McMullen Creek Member is absent at the type section (Fig. 9). The crystal content of the ignimbrite decreases southwards from 10%–15% at the type locality to less than 5% in the Goose Creek basin. Here, the basal ash-fall layer also thickens to 10 m as a result of local sedimentary reworking in a topographic basin.

Interpretation

Sustained subaerial ash fallout from a tall explosive eruption column deposited the extensive lower ash-fall layer. The eruption column then began fountaining (collapsing), generating a sustained, very hot granular fluid–based pyroclastic density current that traveled widely across the Cassia area, depositing intensely welded tuff above the glass transition. The early current was depletive (Kneller and Branney, 1995), becoming fully dilute and cooler distally (~30 km from source), presumably as the result of sedimentation and turbulent admixture of cool atmospheric air. Fluid turbulence-induced tractional deposition below the glass-transition temperature is recorded by the low-angle, cross-stratified, nonwelded tuff in all southern locations. As the mass flux of the sustained explosive eruption waxed, the current became more concentrated and hotter at distal locations, recorded by the upward transition into massive, intensely welded tuff (e.g., at Trapper Creek; Fig. 9). The grading of the vitric lapilli indicates waxing then waning flow competence in the sustained pyroclastic density current that was granular fluid–based (see Branney and Kokelaar 2002; Carrasco-Núñez and Branney, 2005).The southward-diminishing lapilli content of the McMullen Creek ignimbrite also is consistent with a southward-moving, depletive pyroclastic density current (Kneller and Branney, 1995) from a source to the north (McCurry et al., 1996). The vertical changes in the ignimbrite record changes (unsteadiness) in this sustained current, though evidence for significant time breaks during its emplacement is lacking. The very hot current became somewhat cooler during a major incursion of vitric lapilli (the central, less-welded zone of lapilli-tuff). As with underlying members, this cooling may have been the result of the entrainment of large volumes of cooler fragments, or interaction with surface or groundwater that enhanced explosive incorporation of these fragments. This occurred during the time of peak flow (maximum clast size) and may be related to caldera subsidence, after which entrained lapilli decreased in size, with resumption of the very high emplacement temperatures, above the softening point of the rhyolite. Toward the end of the eruption, nonwelded ash fell distally on the ignimbrite sheet prior to cooling.

Lincoln Reservoir Member

The Lincoln Reservoir Member (former "Member 5" of Wright et al., 2002) is the youngest member exposed in the Cassia Hills and is widely distributed. It is a rheomorphic lava-like ignimbrite, ~35 m thick, with a thin basal fall sequence (Fig. 11A). At its type locality (Little Creek section; Fig. 1) it overlies a well-developed, baked orange paleosol in the top of the McMullen Creek Member. The member is succeeded by the Castleford Crossing Member (contact is not seen) and is readily distinguished from other Cassia Formation members by uniquely containing four compositional modes of pyroxene (two augite-pigeonite pairs; Fig. 6). Otherwise, its crystal content (10%–15%; 1–3 mm in size) and mineral assemblage are similar to the other plagioclase feldspar–bearing members.

The basal ash-fall layer is 30 cm thick with parallel crystal- and vitric-rich beds and two layers of clast-supported small pumice lapilli, fused by the overlying ignimbrite (Fig. 11C). The lower vitrophyre of the ignimbrite is perlitic with up to 2-m-long red axiolites along the welding fabric. It is sharply overlain by massive, red-brown, lithoidal tuff, 30 m thick, with an upper, 1-m-thick, vitrophyre. Rheomorphic folds are abundant and divide the ignimbrite into a lower "flat zone" with subhorizontal intrafolial isoclines and sheath folds, and an upper "steep zone" of more open, upright to overturned anticlines and synclines up to 10 m in scale that refold earlier intrafolial isoclines (Fig. 11A). Similar architecture is seen in the Dry Gulch, Grey's Landing (Andrews and Branney, 2011), and Castleford Crossing ignimbrites. In the north (e.g., above Dry Gulch quarry), the basal contact is locally peperitic, with brecciated vitrophyre intermingled with disaggregated (fluidized) substrate sediment (Figs. 9 and 11B). The member thins southward to less than 10 m at Goose Creek (former "upper Goose Creek tuff" of Hackett et al., 1989), and crystal content decreases from 10%–15% to ≤5%.

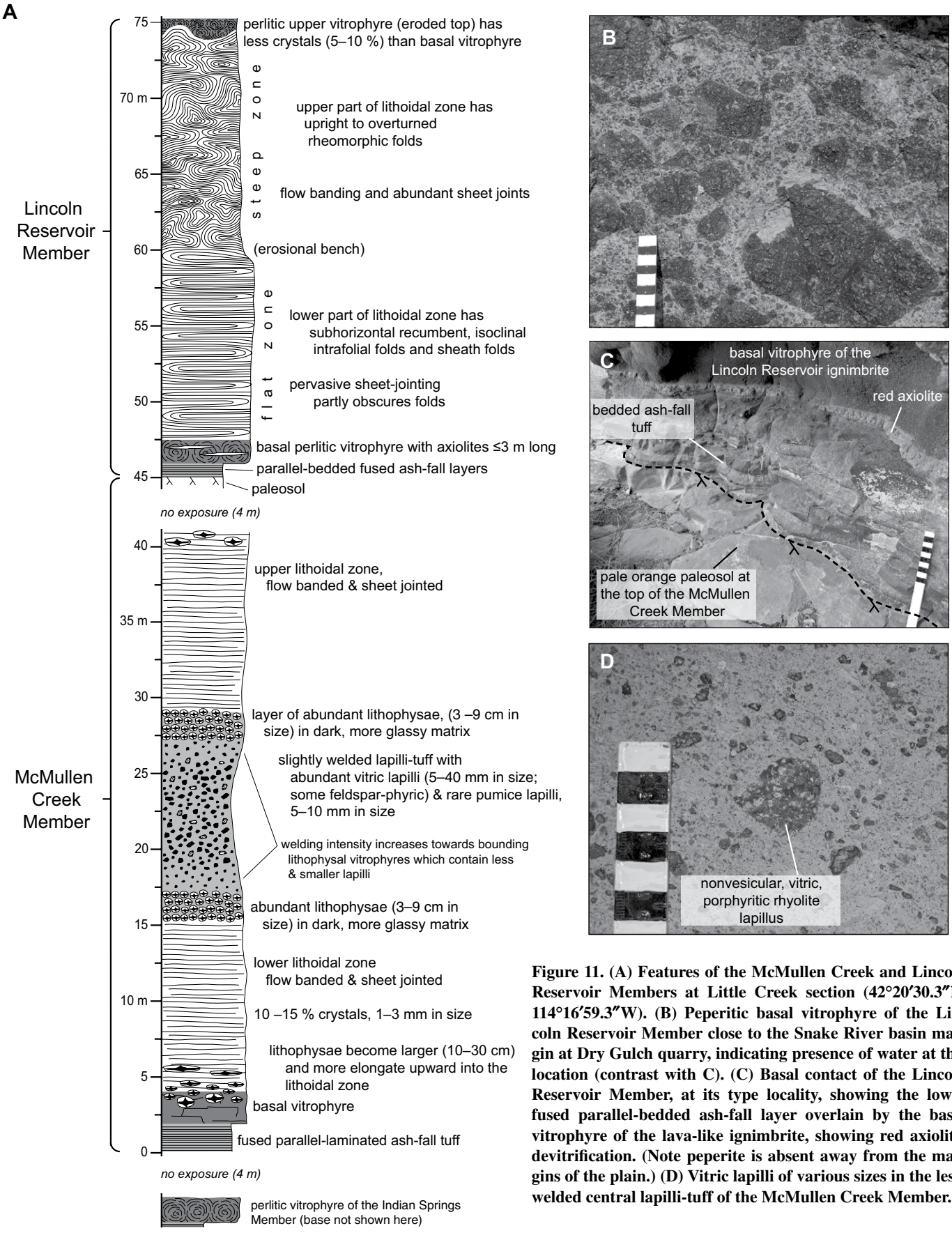

Figure 11. (A) Features of the McMullen Creek and Lincoln Reservoir Members at Little Creek section (42°20′30.3″N, 114°16′59.3″W). (B) Peperitic basal vitrophyre of the Lincoln Reservoir Member close to the Snake River basin margin at Dry Gulch quarry, indicating presence of water at this location (contrast with C). (C) Basal contact of the Lincoln Reservoir Member, at its type locality, showing the lower fused parallel-bedded ash-fall layer overlain by the basal vitrophyre of the lava-like ignimbrite, showing red axiolitic devitrification. (Note peperite is absent away from the margins of the plain.) (D) Vitric lapilli of various sizes in the less-welded central lapilli-tuff of the McMullen Creek Member.

Interpretation

Subaerial fallout from an unsteady plinian eruption column was followed by emplacement of a widespread and protracted pyroclastic density current that was emplaced at temperatures above the rhyolite glass-transition temperature. The ignimbrite is a simple cooling unit with no evidence for significant time gaps during its emplacement. As it aggraded, hot pyroclasts coalesced and sheared into a mylonite-like flow-laminated welded ignimbrite. Shear near the lower flow boundary produced rheomorphic isoclines and sheath folds, and this shear zone rose during aggradation of the deposit (Branney and Kokelaar 1992; Sumner and Branney, 2002). After cessation of the pyroclastic current, rheomorphism continued, with folding in the upper steep zone. The peperitic basal contact in the north indicates that the hot ignimbrite was emplaced onto wet (shallow lacustrine?) substrate with proximity to the Snake River Plain, as with the Wooden Shoe Member.

Castleford Crossing Member

The Castleford Crossing Member ("Castleford Crossing ignimbrite" of Bonnichsen et al., 1989) is a massive lava-like rhyolitic welded tuff that locally exceeds 1350 m in thickness. It is the lowest unit recovered from the 1.9-km-deep Kimberly borehole, ~13 km north of the Cassia Hills (Fig. 12A; Shervais et al., 2013), but its base is best exposed at Castleford Crossing (~48 km to the west; Fig. 12C; Bonnichsen et al., 2008), after which the unit is named. At Kimberly, the tuff is mostly pale gray and lithoidal with sparse blocky vitric fragments less than 6 mm in size (Fig. 12A). This passes up abruptly into an upper vitrophyre, 42 m thick, the uppermost 28 m of which are autobrecciated, with framework-supported blocks, and hydrothermal alteration (Fig. 12A). As with other Snake River–type ignimbrites (Andrews and Branney, 2011), a lower "flat zone" and an upper "steep zone" are marked by the attitude of the welding foliation and rheomorphic fold axial surfaces (Fig. 13B). Within the upper vitrophyre, the foliation is a eutaxitic fabric of welded and deformed glass shards. At Kimberly, the ignimbrite is overlain by 18 m of white, parallel-laminated lacustrine sediment (Fig. 12A). We provide a plagioclase $^{40}Ar/^{39}Ar$ age of ca. 8 Ma for this member (Table 1), though its minimum age is constrained with more precision by our sanidine $^{40}Ar/^{39}Ar$ date of 8.109 ± 0.046 Ma from the overlying Kimberly Member, and it is consistent with a date of 8.19 ± 0.14 Ma (Konstantinou et al., 2012).

Crystal abundance is high (20%–30%, 1–4 mm in size) and consistent throughout the Castleford Crossing Member, with an assemblage of plagioclase, pigeonite, augite, magnetite, and rare quartz. The pyroxenes are particularly distinctive, with higher MgO contents (11.5–16.8 wt%) than any other member of the Cassia Formation (Fig. 6).

At Castleford Crossing, a basal 10-cm-thick, parallel-laminated ash-fall layer overlies a red baked paleosol developed in the upper autobreccia of the Balanced Rock rhyolite lava (Fig. 13D), and the overlying basal vitrophyre of the ignimbrite is nonbrecciated and hydrothermally altered. The ignimbrite is lava-like and highly rheomorphic, with abundant isoclinal to open folds, and abundant sheath folds (Fig. 13E). The ignimbrite is exposed further east in the Cotterel Hills (former "Unit-6 of the Salt Lake Formation"; Konstantinou et al., 2012), and on the north side of the Snake River Plain in the Eastern Bennett Hills (former "Tuff of City of Rocks" of Oakley and Link, 2006). We have correlated these wide-spaced locations (Fig. 12C) on the basis of a combination of: (1) stratigraphic position and geochronology (Table 1); (2) the distinctive, high-Mg augite and pigeonite populations, both of which differ from those of other Snake River ignimbrites (Fig. 6); (3) closely similar whole-rock geochemistry, as seen on various trace-element ratio-ratio plots (e.g., Fig. 7), which is distinct from all other units of similar age; and (4) indistinguishable paleomagnetic thermoremanent magnetization directions (Fig. 12B).

The Castleford Crossing ignimbrite covers ≥14,000 km^2, based on the known exposures and extending to reasonable topographic barriers inferred to have been present during the eruption (Fig. 12C). Using known and inferred thickness variations, we estimate a bulk volume of ~1900 km^3. Thicknesses are poorly constrained in central parts of the plain, although a broadly basinal geometry is inferred, and the ≥1.35 km thickness at Kimberly is the thickest eruption unit recorded in the province. The volume estimate is highly conservative because (1) the borehole clearly does not penetrate the full thickness of the ignimbrite; it does not even encroach a basal vitrophyre or any lithic breccias as might be expected proximally; (2) the ignimbrite is likely to have been emplaced farther west and east along the axis of the Snake River basin; and (3) we have not included any volume for a caldera fill of dimensions similar to those inferred elsewhere in the province, where caldera areas of ~5000 km^2 are proposed (e.g., at Yellowstone and Heise volcanic fields; Christiansen, 2001; Morgan and McIntosh, 2005). Finally, (4) the estimate excludes any expected widespread plinian and coignimbrite ash. The conservative estimate equates to a dense-rock equivalent volume of ~1870 km^3 (measured Castleford Crossing ignimbrite density 2340 kg m^{-3}; magma density of 2380 kg m^{-3} of Ochs and Lange, 1999) and a magnitude of 8.6 (method of Pyle, 2000). The magnitude of this eruption is comparable to other large explosive eruptions in the Yellowstone–Snake River Plain volcanic province (Christiansen, 2001; Morgan and McIntosh, 2005; Ellis et al., 2012).

Interpretation

After a period of repose, an explosive supereruption (Mason et al., 2004; Self, 2006) to the north of the Cassia Hills began with a tall eruption plume (recorded by the stratified ash-fall deposit seen at Castleford Crossing, presumably ~30–50 km from source). This was followed by a hot sustained granular fluid–based pyroclastic density current that aggraded a massive intensely welded, rheomorphic ignimbrite. The current flowed westward along the Snake River basin to beyond Castleford, and eastward across the present-day Cotterel Hills. It also encroached the north flanks of the basin (Mount Bennett Hills), but it did not extend southward over the area of the Cassia Hills, where we infer a topographic high had developed. The eruption was clearly of caldera-forming magnitude (Smith, 1979), and the >1.35-km-thick ignimbrite encountered in the Kimberly borehole may be the first caldera-fill ignimbrite identified in the central Snake River Plain. This interpretation would be consistent with the hydrothermal alteration, and the overlying lacustrine sediments (caldera lake). However, caldera-fill ignimbrites typically contain lithic mesobreccias and megabreccias from rock avalanches and landslides from unstable caldera walls (Lipman, 1984; Branney and Kokelaar, 1994; Troll et al., 2000; Ferguson et al., 2012), and these are not seen in the ignimbrite at Kimberly. Interestingly, mesobreccias and megabreccias are also absent in the 2.5-km-thick rhyolitic succession recovered in the INEL-1 core in the eastern Snake River Plain (Doherty et al., 1979), which may be another thick caldera fill. The absence of breccias in the thick Castleford Crossing ignimbrite at Kimberly (and at INEL-1) may mean that (1) the site is a caldera fill, but relatively distant (tens of kilometers) from the nearest steep, formerly unstable caldera wall scarp (this would indicate the caldera is very large); (2) the core penetrates only the upper part of the fill, with breccias concealed at greater depth (i.e., the caldera was very deep); or (3) the thickness merely reflects ponding in a regional downwarp that developed into the Snake River basin. All three scenarios imply volumes larger than our conservative estimate.

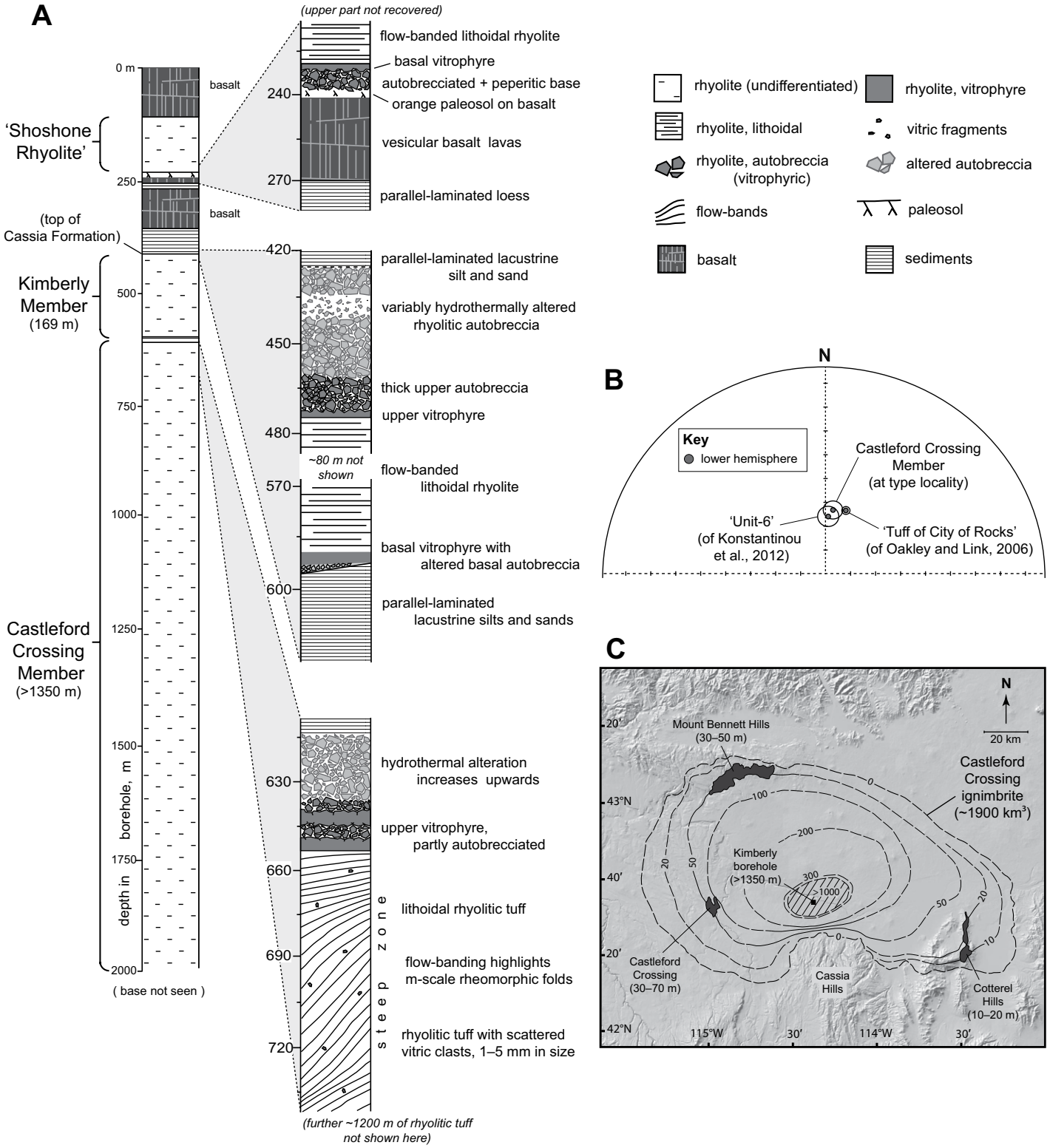

Figure 12. (A) Upper part of the Cassia Formation as revealed in the Kimberly borehole, showing the exceptional thickness of the Castleford Crossing Member. (B) Stratigraphic stereonet showing the indistinguishable site mean paleomagnetic (thermoremanent magnetization) directions for all correlatives of the Castleford Member. For the purpose of correlation, local postdepositional tectonic dips have been removed. (C) Inferred distribution of the Castleford ignimbrite in the central Snake River basin, with known and inferred thickness contours yielding a conservative volume estimate of ~1900 km³.

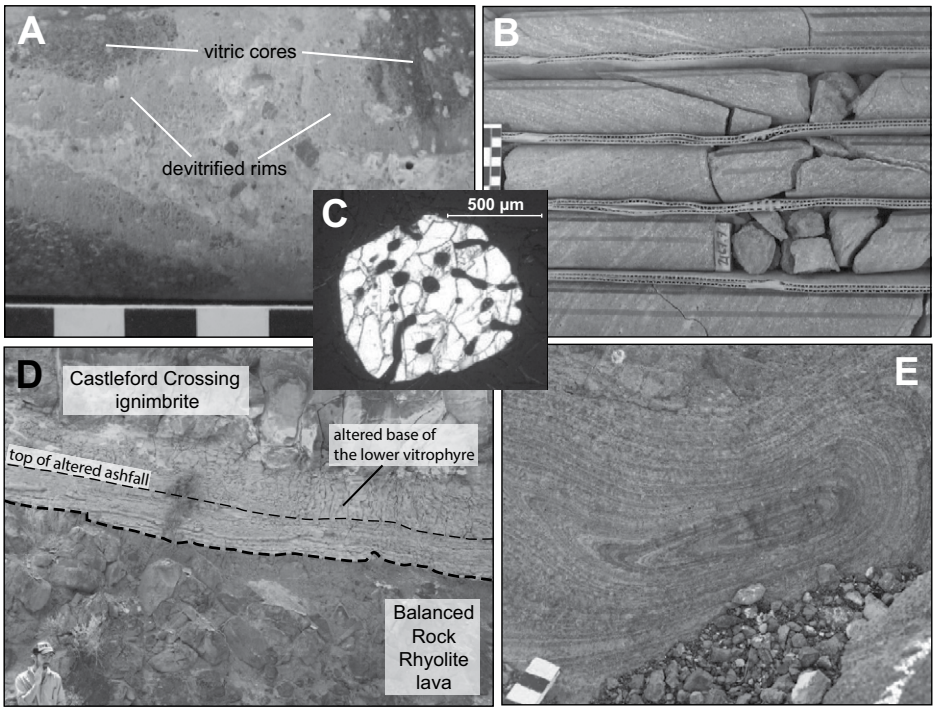

Figure 13. (A) Upper autobreccia of the lava-like rhyolitic Kimberly Member; larger blocks are clast supported with vitric cores and devitrified rims. (B) Castleford Crossing Member (rheomorphic rhyolitic ignimbrite), where changing angle of the flow banding with depth indicates rheomorphic folding within an upper "steep zone." (C) Resorbed quartz crystal, characteristic of the Kimberly Member. (D) Base of the Castleford Crossing Member at its type locality. A red, baked paleosol developed on the upper autobreccia of the Balanced Rock rhyolite block lava is overlain by a parallel-bedded basal ash-fall (white; devitrified) of the Castleford Member, and passes up into the basal vitrophyre of the Castleford Crossing ignimbrite. (E) Sheath fold picked out by flow banding in the rheomorphic Castleford Crossing ignimbrite; extension direction is parallel to centimeter scale.

Kimberly Member

The 8.109 ± 0.046 Ma (Table 1) Kimberly Member is a 169-m-thick, lava-like rhyolitic unit exposed solely in the Kimberly core with no correlatives identified elsewhere (Fig. 12A). A basal vitrophyre, 6 m thick, has an inclined basal contact with the underlying parallel-laminated sediments. The lower 0.4 m of the vitrophyre is brecciated and pervasively altered, and similar bands of alteration, 1–2 cm thick, follow fractures higher within the vitrophyre. The rhyolite everywhere contains 15%–20% crystals (1–4 mm in size) of plagioclase, anorthoclase, sanidine, pigeonite, augite, magnetite, and quartz. The presence of anorthoclase and abundant quartz crystals with strong resorption textures (Fig. 13C) distinguishes it from the other members.

A central lithoidal zone, 119 m thick, is flow banded, with sheeting joints exploiting some of the flow bands. The upper vitrophyre has a lower 1.5-m-thick coherent zone that passes up into a clast-supported autobreccia, 2 m thick, composed of angular vitric clasts (2–10 cm in size) in a reddened oxidized matrix (Fig. 12A). Microscopic, possible welded shards are visible only in the upper vitrophyre, and the unit elsewhere lacks definitive pyroclastic textures. The autobreccia becomes increasingly altered with height, and smaller clasts (≤5 cm in size) are green and devitrified, whereas larger blocks have dark vitric cores and pale devitrified rims (Fig. 13A). The most intense alteration forms a 3-m-thick layer of green clay (between 435 m and 438 m depth; Fig. 12A). Above this, alteration is less intense, even though autobrecciation persists to the top of the unit. The member is directly overlain by parallel-laminated lacustrine sediments, 64 m thick.

Interpretation

The origin of the Kimberly Member as a lava-like ignimbrite or true lava is equivocal in the absence of exposed field relations that show its extent and thickness relationships with topography (e.g., see Henry and Wolff, 1992; Bonnichsen and Kauffman, 1987). Upper autobreccias are not diagnostic, and particle coalescence and rheomorphic attenuation can render some ignimbrites indistinguishable from lavas in thin section (Branney and Kokelaar, 1994). The basal breccia of just 0.4 m thickness is thinner than would be expected at the base of a thick blocky rhyolite lava, and the inclined lower contact in the borehole might be faulted such that a thicker basal breccia is not seen. Conversely, the possibility that the basal contact with lacustrine sediment represents a peperitic base of a lava-like ignimbrite (Branney and Kokelaar, 1994) cannot be excluded, as is seen in the Wooden Shoe and Lincoln Reservoir Members close to the plain margins. The top of the Kimberly Member marks the top of the Cassia Formation.

Shoshone Rhyolite

The Shoshone Rhyolite is the youngest rhyolitic unit in the area. It overlies basalt lavas and sediments above the Cassia Formation, and we provide a $^{40}Ar/^{39}Ar$ age of 6.37 ± 0.44 Ma (Table 1). It is a flow-folded blocky lava, well exposed in the Snake River Canyon, at Shoshone Falls, where it is 200 m thick, with an undulating upper surface composed of autobreccia (Bonnichsen et al., 2008). It contains 10%–15% crystals of plagioclase, pigeonite, augite, magnetite, and trace amounts of quartz. In the Kimberly core, the lava is 120 m thick (Shervais et al., 2013; Fig. 12A), though only the lowermost 30 m section was recovered. At Kimberly, the basal vitrophyre, 8 m thick, has a slightly peperitic autobreccia in contact with the underlying paleosol on older basalt lavas (Fig. 12A).

WHOLE-ROCK AND MINERAL CHEMISTRY

Cassia Formation ignimbrites have SiO_2 contents between 68.3 and 76.1 wt%, Fe_2O_3 between 2.40 and 5.72 wt%, TiO_2 <0.9 wt%, and MgO <1.0 wt% (Table S1, recalculated volatile-free; see footnote 1) with metaluminous A-type rhyolitic signatures typical of most other Snake River–type ignimbrites in the region (e.g., Bonnichsen and Citron, 1982; Wright et al., 2002; Cathey and Nash, 2004; Andrews et al., 2008; Bonnichsen et al., 2008; Ellis et al., 2010). Whole-rock concentrations of major and trace elements are remarkably consistent within each individual member, with minimal variations with height (e.g., <1 wt% SiO_2), and only slightly more variation laterally (e.g., SiO_2 in the Lincoln Reservoir Member varies by 1.8 wt%). This has been previously reported for many other central Snake River Plain ignimbrites and

seems to be a common feature (e.g., Bonnichsen et al., 2008; Ellis et al., 2013).

Bulk silicate earth–normalized (after McDonough and Sun, 1995) trace-element data of all members follow closely similar patterns with high Rb, Th, U, and Pb abundances, and negative Ba, Nb, and Sr anomalies (Fig. 7, inset), which are most pronounced in the older members (e.g., Magpie Basin and Big Bluff Members). Despite this, the individual members can be distinguished from each other on a ratio plot of Rb/Sr versus Th/Nb (Fig. 7), where each member defines a distinct chemical field that is readily distinguishable from enclosing members.

Stratigraphic Variations in Whole-Rock and Mineral Chemistry

Using the stratigraphy outlined earlier herein, the Cassia Formation is seen to record systematic variations in both major- and trace-element chemistry with time (Fig. 14; Table S1 [see footnote 1]): SiO_2, Rb, La, and Th decrease systematically with stratigraphic height, whereas TiO_2, CaO, Fe_2O_3, MgO, Sr, Ba, and Zr all increase. This trend then "resets" at the Dry Gulch Member, which has some chemical similarities (e.g., elevated SiO_2 and low TiO_2) with the older Magpie Basin and Big Bluff Members, and the trend repeats with height through the overlying members (Fig. 14). These trends are matched by systematic changes in pyroxene composition with stratigraphic height: Pyroxene Mg-numbers increase up the succession (Fig. 14), indicating crystallization from successively more Mg-rich magmas. Magmatic temperature estimates from equilibrium pyroxene pairs (QUILF algorithm of Andersen et al., 1993) show that, with the exception of the Magpie Basin Member, early Cassia Formation units (Big Bluff–Little Creek) record indistinguishable temperatures of ~900 °C (Fig. 15). Conversely, temperature estimates from the Dry Gulch to Castleford Crossing Members suggest a trend of increasing temperature with stratigraphic height (Fig. 15), which may account for the increasing pyroxene Mg-numbers due to crystallization from progressively hotter magmas. Also of note is that the resetting of whole-rock and mineral trends between the Little Creek and Dry Gulch Members is also associated with an abrupt decrease in estimated magmatic temperature (Fig. 15). A second reset is also exhibited by the higher-silica Kimberly Member, which also corresponds with an abrupt drop in magmatic temperature. The Cassia Formation may therefore record repeated geochemical cycles, each trending toward less-evolved rhyolite compositions with time separated by abrupt shifts to more-evolved compositions, and cooler magmatic temperatures.

Broadly similar chemical variations in Snake River successions elsewhere are thought to reflect a province-wide trend toward less-evolved compositions over time (e.g., Nash et al., 2006; Bonnichsen et al., 2008). However, the abrupt chemical (and mineralogical) shifts of the Dry Gulch and Kimberly Members have not been recognized. Similar geochemical and mineralogical trends have also been noted within the Rogerson Formation further west (Knott et al., 2016), where newly described abrupt shifts in composition are remarkably similar to those seen in the Cassia Formation.

Origin of Temporal Chemical Variations within the Cassia Formation

We explore the origin of the recurrent chemical cycles (Fig. 14) within the Cassia Formation in the context of current petrogenetic models for Snake River Plain rhyolites (e.g., McCurry and Rodgers, 2009). Explanations for the chemical progression toward less-evolved rhyolite compositions in the Snake River Plain over time have been limited: Suggestions have invoked the competing effects of recharge of magma reservoirs versus differentiation within the magmatic source (Bonnichsen et al., 2008). The rhyolites are thought to be the product of crustal melting (e.g., Cathey and Nash, 2004; Nash et al., 2006; Boroughs et al., 2012; Ellis et al., 2013), with uprising mantle-derived basalt providing the thermal energy (Leeman et al., 2008). Crust available for melting was Archean overlain by Proterozoic to Mesozoic

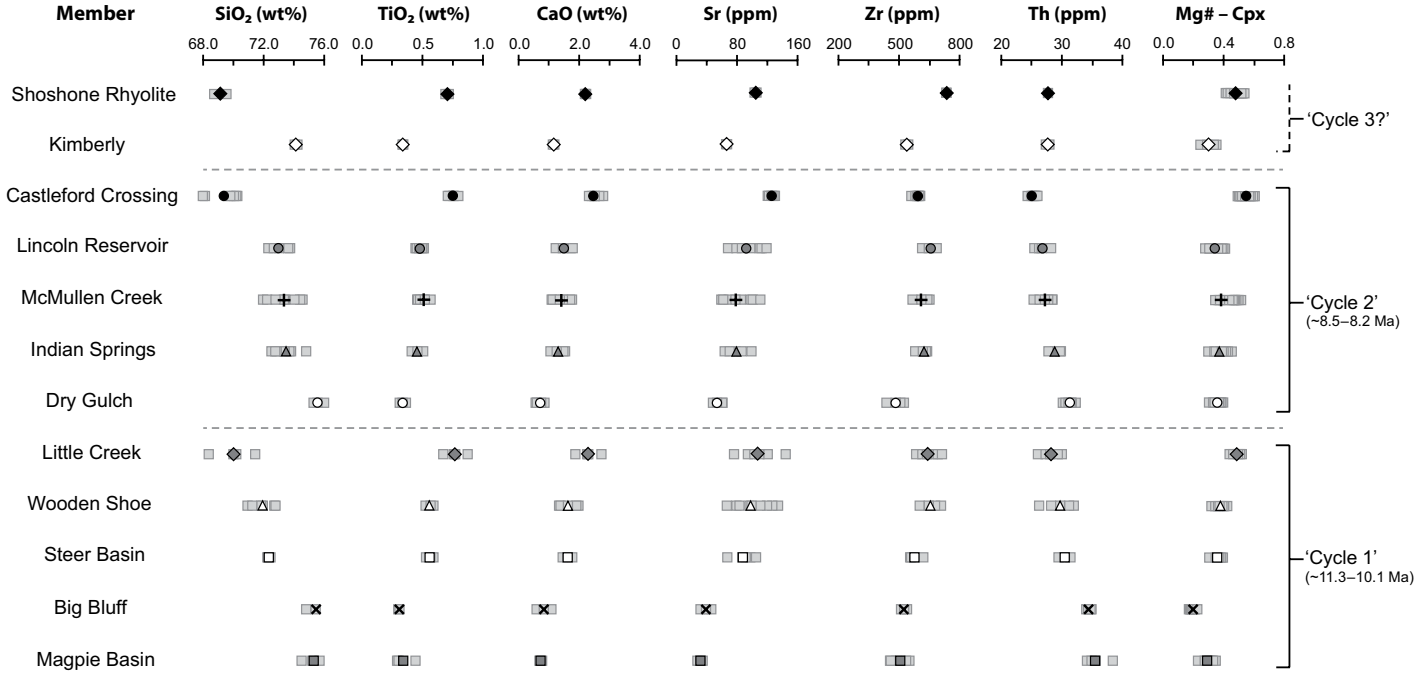

Figure 14. Whole-rock major- and trace-element trends with height through the Cassia Formation. Variations define two to three cycles, each becoming less evolved with time (e.g., decreasing SiO_2, and increasing TiO_2 and CaO). Cpx—clinopyroxene.

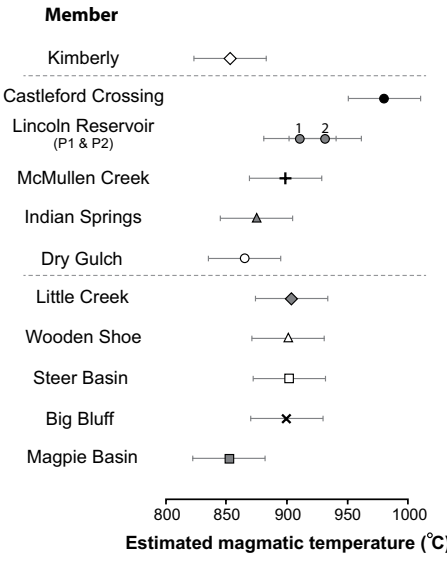

Figure 15. Magmatic temperature estimates (with conservative 30 °C uncertainties) from equilibrium pyroxene pairs (n = ≥5) using the QUILF algorithm of Andersen et al. (1993). Pressure is fixed at 0.5 GPa (as preferred by Cathey and Nash, 2004, 2009). Older members of the Cassia Formation mostly share an indistinguishable temperature of ~900 °C, followed by a trend toward increasing temperatures in the younger units. These are separated by abrupt shifts to lower temperatures (e.g., Dry Gulch Member), which may be due to cyclic petrogenetic processes.

metasediments and Cretaceous to Eocene intrusions; however, Nd isotopes indicate the more ancient components contributed little to the rhyolites (Leeman et al., 2008). The remarkable low $\delta^{18}O$ value of Snake River–type rhyolites is consistent with voluminous melting of hydrothermally altered low $\delta^{18}O$ crustal sources, though how and where this occurred remain controversial (Boroughs et al., 2005, 2012; Bindeman et al., 2008; Drew et al., 2013). Repeated injections of mantle-derived basalt are thought to have ascended through the crust beneath the Snake River Plain until the magmas ponded in large volume at levels of neutral buoyancy in the midcrust (Fig. 16; Bonnichsen et al., 2008; McCurry and Rodgers, 2009). This is consistent with work further east, where seismic P-wave velocity data indicate the presence of a 10–25-km-thick mafic sill complex at ~15 km depth (Peng and Humphreys, 1998; Shervais et al., 2006). In proposed petrogenetic models, $^{143}Nd/^{144}Nd$ ratios of Snake River Plain rhyolites indicate mixing between mantle and crustal components. However, estimates of the total mantle contribution vary from 10%–60% (Nash et al., 2006; McCurry and Rodgers, 2009) to ≥80% (Wright et al., 2002) depending on model parameters. Mantle- and crustal-derived materials likely underwent melting, assimilation, storage, and homogenization (MASH; see Hildreth and Moorbath, 1988; Fig. 16) in the midcrust, which subsequently generated an isotopically hybridized source region (McCurry and Rodgers, 2009). Partial melts produced from this midcrustal source region are inferred to have been primitive (low SiO_2, high MgO) rhyolitic magmas, and these ascended to shallower magma reservoirs, where they underwent differentiation (Fig. 16). We propose that the controlling factors in the Cassia Formation chemical trends were (1) progressive evolution of a midcrustal source region, coupled with (2) subsequent fractionation of the rhyolitic magmas in upper-crustal reservoirs (see following), and followed by (3) the migration of the magmatism into a new, more pristine region of midcrust, with the initiation of a new cycle .

Thermal and Chemical Evolution of a Midcrustal Hybrid Source Region

The cyclic chemical trends toward less-evolved compositions exhibited by the Cassia Formation may reflect the temporal evolution of a midcrustal source region. During the early stages of basaltic intraplating, batches of silicic melt are generally produced by small degrees of crustal melting and the incomplete crystallization of the intruded mafic magmas (Annen, 2011). In the central Snake River Plain, melts generated during this stage were likely high in silica, similar to the composition of the Magpie Basin and Big Bluff Members (stage 1 in Fig. 16). However, as the emplacement rate of mantle-derived basalt progressively increased, the repeated injections caused the temperature in the source region to rise, resulting in an increase in the degree of melting (cf. Annen, 2011), so that successively formed melts would be less differentiated with time (e.g., stage 2 in Fig. 16). This chemical evolution of the melt composition is the reverse of that predicted by crystal fractionation. The trend to less-evolved rhyolites, seen between members of the Cassia Formation, could alternatively record melting of an increasingly refractive, residual source (Leeman et al., 2008); however, this mechanism does not readily account for the very large volume of the less-evolved Castleford Crossing Member, as it would become increasingly difficult to melt sufficient volumes of an increasingly refractory source. We therefore infer that the injected mafic magmas contributed directly to melt batches ascending from an increasingly hybridized source region, resulting in progressively less-evolved but voluminous rhyolites.

The abrupt chemical shifts to more-evolved compositions (e.g., the Dry Gulch Member and later the Kimberly Member) may record the migration of magmatism into a more pristine region of the crust, less inundated by basaltic magmas, thus producing a higher-silica rhyolite. This may be related to the migration of the North American plate over the quasi-stationary Yellowstone hotspot. Once the shift to a new crustal location occurred, a second petrogenetic cycle began (recorded in the succeeding trend toward less-evolved compositions, exhibited by the overlying members) as the crust became increasingly hybridized by the injection of mantle-derived basalt. However, in both cycles, Zr content increases up the succession (Fig. 14). This is inconsistent with the increased influx of basaltic (low Zr) material, which would dilute Zr concentration. Therefore, in order to explain the Zr trends, we explore the role of crystal fractionation after the melts ascended from their midcrustal source.

Degree of Fractional Crystallization

Compatible and incompatible trace-element ratios (Fig. 17) show that many members of the Cassia Formation define a common field, whereas others (e.g., Magpie Basin Member) deviate from this field, with higher La/Ba and Th/Zr. If the low-silica members in the common field are assumed to represent primitive rhyolitic melts, originating from the midcrustal source region, then their La/Ba and Th/Zr ratios are broadly consistent with ~30% melting of a hybrid dioritic source (Fig. 17) as proposed by McCurry and Rodgers (2009). We also assume that trace amounts of zircon (constrained to ≤0.5% based on model calculations) were present in the source region during melting, in order to establish appropriate Th/Zr ratios. This is consistent with the presence of inherited Proterozoic (ca. 1.4 Ga) zircons in several Cassia Formation members (McMullen and Little Creek Members; Table S4 [see footnote 1]).

The deviation of the more silicic members from the common field (Fig. 17) can be explained by small degrees (≤5%) of fractional crystallization within shallower, upper-crustal, magma reservoirs, with an assemblage consisting of plagioclase, K-feldspar, clinopyroxene, and trace amounts (~1%) of zircon. Evidence for the fractionation of zircon is (1) the ubiquitous presence of phenocrystic (rather than solely inherited) zircons in all Cassia Formation members (Table S6; see footnote 1), and (2) higher Th/Zr ratios in the more silicic members (Fig. 17), which are readily explained by zircon fractionation. The progressive trends from lower to higher Zr contents with stratigraphic height in each cycle (e.g., Magpie Basin–Little Creek

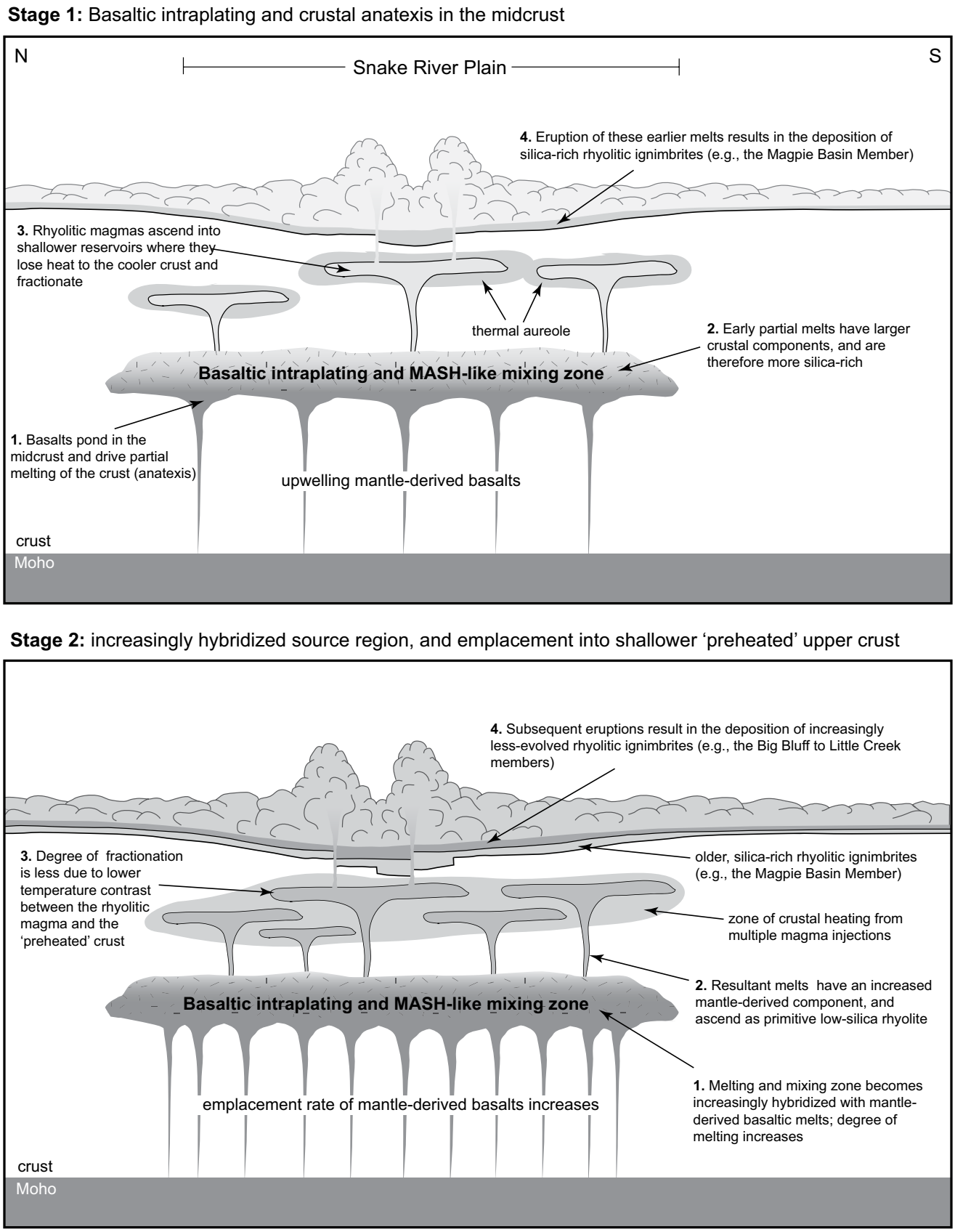

Figure 16. Petrogenetic model for the central Snake River Plain illustrating the potential cause of the repetitive geochemical trends observed in the Cassia Formation. MASH—melting, assimilation, storage, and homogenization.

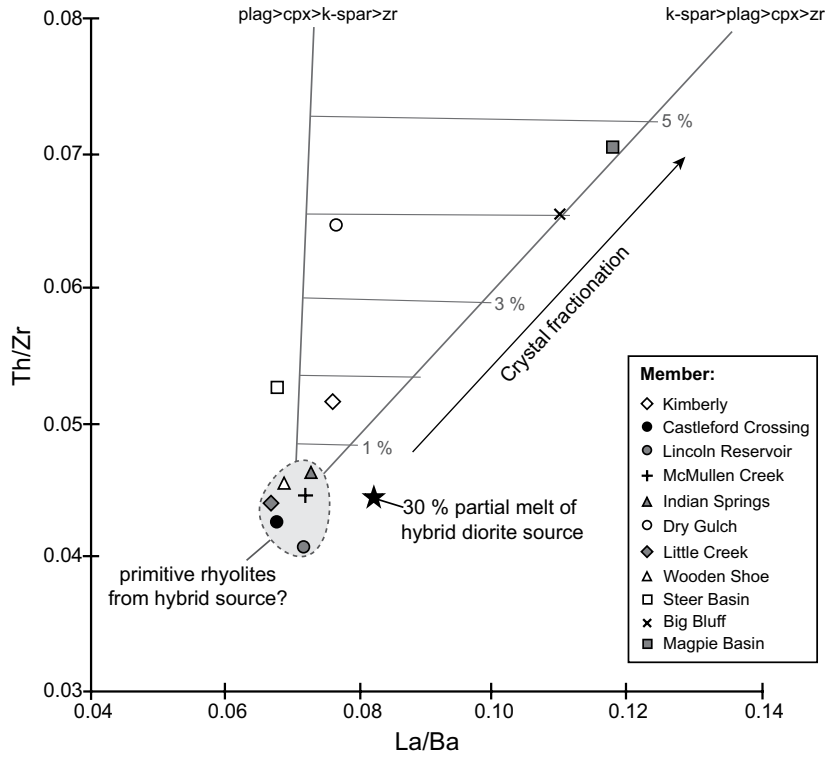

Figure 17. La/Ba vs. Th/Zr plot; note that most members of the Cassia Formation define a common field (gray). If this field is assumed to represent more primitive rhyolite that originated from a midcrustal hybrid source region, then deviation from this field may reflect small degrees of fractional crystallization (Fig. 16). Abbreviations: k-spar—K-feldspar; plag—plagioclase; cpx—clinopyroxene; zr—zircon.

Members; Fig. 14) are inferred to record progressively smaller degrees of fractionation with time. The recurrent emplacement of melt batches into upper-crustal reservoirs would generate thermal aureoles, and progressively heat the surrounding crust (Annen, 2011; stage 1 in Fig. 16). The result would be a reduction in the temperature contrast between the later, more-primitive lower-silica melt batches and the surrounding crust, thus hindering the fractionation of successive melt batches emplaced into this preheated crust (stage 2 in Fig. 16). This may account for the progressively smaller degrees of fractionation necessary to generate the upward trend toward less-evolved compositions seen through the Cassia Formation. Estimated magmatic temperatures for Snake River rhyolites (e.g., Andrews et al., 2008; Bonnichsen et al., 2008; Ellis et al., 2010) also show signs of increasing with time during a cycle, which is consistent with progressively lower degrees of heat loss.

The more-evolved Dry Gulch Member marks the start of the second cycle. We infer that the magma ascended and ponded in a new location of (non-preheated) upper crust, where it began to cool and crystallize (see Fig. 16). The shift to a new location also was accompanied by a longer repose period (~1.6 ± 0.2 m.y.; Table 1), during which some cooling of the upper crust may have occurred. The overlying members then erupted in relatively quick succession (e.g., six eruptions within ~0.8 m.y.; Table 1), thus allowing less time for fractionation and resulting in ignimbrites with compositions closely similar to the source primitive rhyolite (Fig. 17). This interpretation would benefit from more refined age data.

We infer that both mechanisms 1 and 2 operated in tandem, and that progressive hybridization of the source region was the primary control on the observed trends in the Cassia Formation, with small degrees of upper-crustal crystal fractionation (in particular zircon fractionation) serving to modify the observed Zr trends. These mechanisms are compatible with acquiring the low $\delta^{18}O$ signature during crustal melting, be this hydrothermally altered granite (Boroughs et al., 2005, 2012) or caldera sources (Bindeman et al., 2008). Available $^{87}Sr/^{86}Sr$ data (Wright et al. 2002) are also broadly consistent with these petrogenetic interpretations, with the least-evolved members (e.g., Little Creek Member) having ratios closer to Snake River basalts than the more-evolved members (e.g., McMullen Creek Member). However, we emphasize the need for more isotopic data that are more robustly constrained within the new eruption-unit stratigraphy described herein.

The recurrent emplacement of large volumes of mantle-derived basalt beneath the central Snake River Plain would have fundamentally altered the structure of the crust. This likely played a role in the structural evolution of the Snake River basin, and the flexure of its northern and southern flanks, including the northern margin of the Cassia Hills (see following).

SUBSIDENCE OF THE SNAKE RIVER BASIN BY BASALTIC INTRAPLATING DURING BASIN AND RANGE EXTENSION

In this section, we explore how the structure of the Cassia Hills records the effects of wholesale modification of the continental crust in southern Idaho by voluminous basaltic intraplating, heating, and hybridization. We use the new, dated volcanic stratigraphy to provide constraints on the mid-Miocene deformational history of the area during the period of intense magmatism and crustal modification.

The central to eastern Snake River plain is an ENE-trending intracontinental basin, 600 km long and 100 km wide, which we refer to as the Snake River basin (Fig. 1). It has a mid-Miocene to recent volcanic and volcaniclastic fill of at least 5 km thickness (Champion et al., 2002; McQuarrie and Rodgers, 1998) and is flanked to the north and south by elevated massifs (Fig. 1) that expose regional, basin-bounding monoclines. Along the northern margin of the basin, rhyolitic strata dip southward, and regionally, subhorizontal fold hinges within the Mesozoic basement plunge southward by as much as 25° (McQuarrie and Rodgers, 1998). The opposing southern monocline trends approximately NE-SW and is exposed in the north of the Cassia Hills (Cassia monocline; Fig. 18). The monoclines are the structural manifestation of Snake River basin subsidence, which has been attributed to the emplacement and cooling of a vast midcrustal mafic intrusion (Sparlin et al., 1982; Leeman et al., 2008). This subsidence was possibly accommodated by the lateral flow of heated lower crust into north and south flanking regions, which were undergoing concurrent Basin and Range extension (McQuarrie and Rodgers, 1998). It is generally believed that the subsidence, like the volcanism, was time-transgressive and migrated eastward with time toward Yellowstone (Pierce and Morgan, 1992;

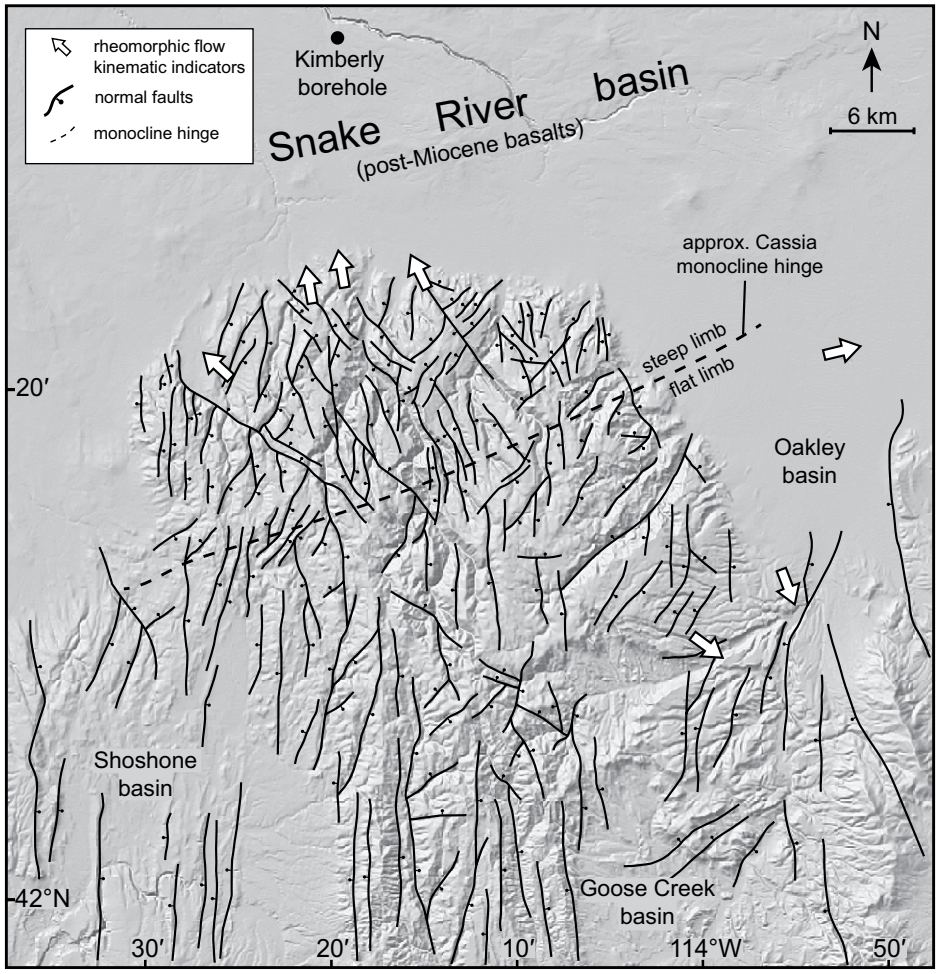

Figure 18. Digital elevation model of the Cassia Hills showing major fault trends, kinematic rheomorphic transport directions, and the approximate location of the Cassia monocline hinge. Note that faults in the southern Cassia Hills trend predominantly N-S, whereas faults in the north trend both NE and NW.

Beranek et al., 2006). However, there are few constraints on its timing and evolution, and most structural work has been done in the east. Structural considerations of ignimbrites in the Cassia Hills area provide useful constraints in the central Snake River Plain area. The Cassia Hills record both mid-Miocene E-W extension and northerly subsidence. The range is an intensely faulted structural dome covering 1500 km^2, with a relief of ~1100 m and strata dipping outward, to the west, north, and east.

Basin and Range

E-W Basin and Range extension is recorded by numerous close-spaced (~3 per km), high-angle faults with small (tens to hundreds of meters) offsets, and associated gentle tilting of the narrow fault blocks. The trend of the Basin and Range faults is N-S, with some ranging from NNW to NNE (Fig. 18). N-trending Basin and Range grabens bound the Cassia Hills to the west (the Shoshone basin) and east (the Oakley basin). Most of the N-trending faults cut the entire Cassia Formation, although some older faults cut only the basement. Examination of thickness variations of ignimbrites provides information on the timing of early Basin and Range extension. For example, the extension produced N-trending, narrow ridges in the NE Cassia Hills that were not surmounted by the ca. 10.9 Ma Big Bluff Member, whereas younger Miocene units bury these features (Williams et al., 1990). This is consistent with the overall eastward migration of Basin and Range extension across the Snake River region with time (Rodgers et al., 2002).

The northern part of the Cassia Hills is also cut by prominent NW-trending high-angle faults. We relate these to the 11.5–3 Ma opening of the western Snake River rift (Wood and Clemens, 2002) as they are parallel to, and along strike of, its faulted eastern margin (Fig. 1).

A second set of high-angle faults in the northern Cassia Hills trends NE (Fig. 18). These faults do not persist into the southern Cassia Hills and are interpreted here to have formed by brittle outer-arc extension during flexure along the NE-trending Cassia monocline. Elsewhere along the Snake River basin, similar faults have been related to flexure during subsidence (Rodgers et al., 2002).

Cassia Monocline

Cassia Formation ignimbrites preserve information about topographic slopes in the form of thickness variations and paleoflow indicators, and they have been dated to constrain the age of the evolving paleotopography that they bury. We infer that the Cassia monocline had little paleotopographic expression from 10.952 ± 0.010 Ma to 10.139 ± 0.006 Ma, because the Big Bluff, Steer Basin, and Wooden Shoe Members do not thin appreciably up the steep limb of the monocline (Fig. 19). The units simply show gradual tapering toward their distal margins south of the Cassia Hills into the Goose Creek basin. In contrast, the younger Little Creek ignimbrite thins markedly southward from >30 m at the northernmost margin of the Cassia Hills, and pinches out ~8 km south of the Little Creek section (Fig. 19). The limited southward transport of the Little Creek pyroclastic density current was probably influenced by a topographic high near the present location of the monocline hinge (Fig. 18). The overlying Dry Gulch ignimbrite shows marked southward thinning associated with the monocline: It is ~45 m thick at Dry Gulch quarry and rapidly thins to zero across 15 km. The younger Indian Springs ignimbrite also has a distinct "wedge-like" geometry and pinches out ~2 km south of the Little Creek section (Fig. 9). These three ignimbrites have an offlap relationship with respect to the southern margin of the Snake River basin (Fig. 19), and this indicates progressive steepening of the bounding Cassia monocline between ca. 10 and 9 Ma (Table 1).

The succeeding two ignimbrites (McMullen Creek and Lincoln Reservoir Members) do not continue the offlap pattern: They do not pinch out up the monocline, and they extend broadly across the entire Cassia Hills to the south (Figs. 9 and 19). This suggests that between ca. 9 and 8.3 Ma (Table 1), the topography at the southern margin of the Snake River basin had become more subdued, with little topographic expression of the monocline to arrest the advancing pyroclastic density currents.

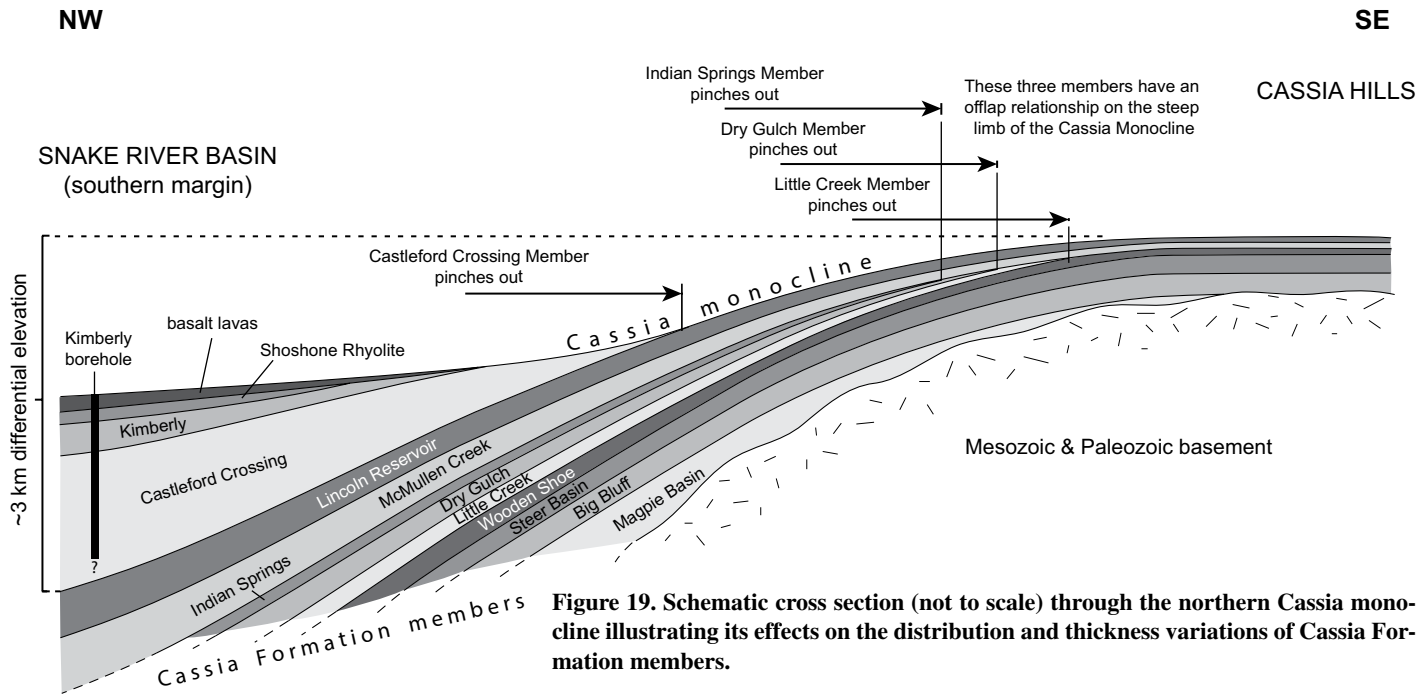

Figure 19. Schematic cross section (not to scale) through the northern Cassia monocline illustrating its effects on the distribution and thickness variations of Cassia Formation members.

Basin subsidence resumed after ca. 8.3 Ma, yielding the present ≥3000 m difference in elevation of the Lincoln Reservoir Member between the top of the Cassia Hills (2400 m above sea level) and the Snake River basin, where it underlies the younger 1.9-km-thick ponded volcanic succession in the Kimberly borehole (Fig. 19). However, a component of this subsidence may have been by caldera collapse (see Branney et al., 2008).

The Cassia monocline is therefore interpreted as a growth structure, recording a protracted mid-Miocene subsidence history of the Snake River basin. A similar subsidence history is also recorded by the Brown's Bench monocline, ~50 km further west, where ignimbrites show a similar offlap relationship with the developing monocline (Knott et al., 2016). An irregular basement high within the Cassia Hills was already evident prior to 11.337 ± 0.008 Ma where the Magpie Basin Member rests unconformably upon the basement in the north, yet it did not surmount the basement barrier to enter the Trapper and Goose Creek basins (Fig. 19). It remains unclear whether the topography at this time was related to early basin-margin flexure, or to Basin and Range extension, which is thought to have preceded the volcanism.

Synvolcanic Topography and Volcano Location

The present study suggests that the source regions of the large rhyolitic eruptions of the central Snake River were topographically depressed relative to the elevated basin margins. Initial regional uplift by impingement of the mid-Miocene hotspot, with accompanying thermal and magmatic modification of the cratonic crust, may be expected (Lowry et al., 2000; Beranek et al., 2006), similar to the present elevated Yellowstone Plateau (Pierce and Morgan, 1992). This may partly account for the sub-Miocene unconformity in the Cassia Hills, although the unconformity may record a component of uplift due to Basin and Range extension.

Locations of the source volcanoes within the Snake River basin are unknown, but patterns of rheomorphic lineations in Cassia Formation ignimbrites have been cited as evidence for a single, common volcanic center at Twin Falls (McCurry et al., 1996). Reexamination of the rheomorphic evidence permits a new interpretation: Kinematic indicators (including delta and sigma objects, fold vergence, imbrication, and inclined stretched vesicles; Branney et al., 2004) are associated with the lineations in the McMullen Creek and Lincoln Reservoir Members, and they show top-to-the-N rheomorphic transport along the northern margin of the Cassia Hills (Fig. 18). They indicate the existence of north-facing topographic slopes—toward the Snake River basin—at the time that the ignimbrites were emplaced. This is consistent with the ignimbrite thickness and offlap relations (described earlier herein) and also with the local occurrences of peperites restricted to the northernmost outcrops of the Cassia Hills, which suggest that aqueous basinal conditions occurred at the southern margin of the Snake River basin during the eruptions (Branney et al., 2008; Fig. 11B). Therefore, we propose that the "fan-like" rheomorphic lineation patterns in the Cassia Hills (McCurry et al., 1996) do not record flow directions away from a single elevated source region as was originally inferred. Rather, the rheomorphic transport was northward, down the slope of the developing Cassia monocline. The more E-W–trending lineations likely record transport influenced by E- and W-tilted Basin and Range graben slopes, as clearly demonstrated by analysis of rheomorphic structures further west (Andrews and Branney, 2011). We conclude that the major explosive eruptions were sourced somewhere within an actively subsiding Snake River basin, and that there is presently no clear evidence that the different ignimbrites of the Cassia Formation erupted from a common eruptive center. The basinal source location of the large explosive eruptions in the central Snake River Plain is in marked contrast to the elevated source of more recent explosive eruptions from the Yellowstone Plateau.

Subsidence and the Magmatic Cyclicity

The youngest eruption unit (Little Creek Member) of the first magmatic cycle in the Cassia area is thought to record the peak of basaltic intraplating, and it was immediately preceded by a phase of Snake River basin subsidence registered by steepening of the Cassia monocline. This subsidence continued, causing offlap of the overlying two ignimbrites (Dry Gulch and Indian Springs Members), and it appears to have

ceased prior to the eruption of the McMullen Creek Member. Basaltic intraplating during the second cycle is thought to have peaked prior to the eruption of the Castleford Crossing Member. This was, again, marked by renewed subsidence, causing the topographic restriction of that ignimbrite against the southern margin of the Snake River basin. It seems crustal subsidence in the central Snake River area was inherently linked to the magmatic cyclicity.

CONCLUSIONS

(1) The Cassia Formation in southern Idaho records 12 major explosive rhyolitic eruptions related to the Yellowstone hotspot between ca. 11.3 Ma and ca. 8.1 Ma. They average 1 per 270 k.y., which is twice the eruption frequency of Yellowstone.

(2) Despite the close similarity of the paleosol-bounded eruption units (all are Snake River type, with ash-fall layers and intensely welded rheomorphic ignimbrites containing abundant blocky vitric fragments and few lithics), each unit can be carefully distinguished using a combination of field, chemical, mineralogical, geochronological, and paleomagnetic characteristics.

(3) The newly defined Castleford Crossing Member records a new supereruption conservatively estimated to be ~1870 km^3 dense rock equivalent, with an eruption magnitude of 8.6. This is similar in scale to recent eruptions at Yellowstone (Christiansen, 2001) and others in the central Snake River area (Ellis et al., 2012). The ignimbrite exceeds 1.35 km in thickness in a proximal (caldera-like) depocenter, and it covers a region ≥14,000 km^2.

(4) Three chemical cycles each record a trend toward less-evolved rhyolitic compositions with time followed by an abrupt return to more-evolved compositions. Each cycle is inferred to record increasing basaltic intraplating and hybridization of the midcrust, with shallower crystal fractionation in upper-crustal reservoirs, and each cycle ended when the magmatism migrated to a new, pristine region of midcrust (starting a new cycle).

(5) The newly defined regional Cassia monocline records incremental subsidence of the vast ENE-trending intracontinental Snake River basin during successive large explosive eruptions. The subsidence history of the basin is recorded by ignimbrite thickness variations, offlap relations, and rheomorphic kinematic indicators, and it is thought to relate to gradual crustal modification associated with the inferred magmatic cycles.

(6) At the time of the eruptions, the source volcanoes were located in a topographically depressed, basinal setting. This is in contrast with the present-day elevated Yellowstone Plateau. There is as yet no evidence that the eruptions recorded by the Cassia Formation had a common source volcano or eruptive center (e.g., at Twin Falls; cf. Pierce and Morgan, 1992; McCurry et al., 1996).

ACKNOWLEDGMENTS

This work was funded by Natural Environment Research Council (UK) grants RP14G0070 and IP-1311-0512. Drilling of the Kimberly borehole was funded by ICDP and U.S. Department of Energy. The Quaternary Dating Laboratory (Denmark) is funded by a grant from the Villum Foundation to Michael Storey. We particularly thank Bill Bonnichsen and Mike Perkins for many useful discussions in the field, John Shervais, Eric Christiansen, and the entire *HOTSPOT* team, and Richard Hinton for assistance on the Edinburgh ion microprobe. We also thank reviewers Bill Leeman and John Wolff, whose comments greatly improved the final manuscript, Butch and Dave Schwarz for logistical help, and our field/laboratory assistants Liam McDonnell, Anne Batz, Mirja Heinrich, Alexander Holst, Fabian Wadsworth, Mark Baldwin, and Juliana Troch, who were great assets.

REFERENCES CITED

Andersen, D.J., Lindsley, D.H., and Davidson, P.M., 1993, QUILF: A Pascal program to assess equilibria among Fe-Mg-Mn-Ti oxides, pyroxenes, olivine, and quartz: Computers & Geosciences, v. 19, p. 1333–1350, doi:10.1016/0098-3004(93)90033-2.

Andrews, G.D.M., and Branney, M.J., 2011, Emplacement and rheomorphic deformation of a large rhyolitic ignimbrite: Grey's Landing, southern Idaho: Geological Society of America Bulletin, v. 123, p. 725–743, doi:10.1130/B30167.1.

Andrews, G.D.M., Branney, M.J., Bonnichsen, B., and McCurry, M., 2008, Rhyolite ignimbrites in the Rogerson graben, southern Snake River Plain volcanic province: Volcanic stratigraphy, eruption history and basin evolution: Bulletin of Volcanology, v. 70, p. 269–291, doi:10.1007/s00445-007-0139-0.

Annen, C., 2011, Implications of incremental emplacement of magma bodies for magma differentiation, thermal aureole dimensions and plutonism–volcanism relationships: Tectonophysics, v. 500, no. 1, p. 3–10, doi:10.1016/j.tecto.2009.04.010.

Armstrong, R.L., Leeman, W.P., and Malde, H.E., 1975, K-Ar dating of Quaternary and Neogene volcanic rocks of the Snake River Plain, Idaho: American Journal of Science, v. 275, p. 225–251, doi:10.2475/ajs.275.3.225.

Beranek, L.P., Link, P.K., and Fanning, C.M., 2006, Miocene to Holocene landscape evolution of the western Snake River Plain region, Idaho: Using the SHRIMP detrital zircon provenance record to track eastward migration of the Yellowstone hotspot: Geological Society of America Bulletin, v. 118, p. 1027–1050, doi:10.1130/B25896.1.

Bindeman, I.N., Fu, B., Kita, N.T., and Valley, J.W., 2008, Origin and evolution of silicic magmatism at Yellowstone based on ion microprobe analysis of isotopically zoned zircons: Journal of Petrology, v. 49, p. 163–193, doi:10.1093/petrology/egm075.

Bonnichsen, B., and Citron, G.P., 1982, The Cougar Point Tuff, southwestern Idaho and vicinity, *in* Bonnichsen, B., and Breckenridge, R.M., eds., Cenozoic Geology of Idaho: Idaho Bureau of Mines and Geology Bulletin 26, p. 255–281.

Bonnichsen, B., and Godchaux, M.M., 2002, Late Miocene, Pliocene, and Pleistocene geology of southwestern Idaho with emphasis on basalts in the Bruneau–Jarbidge, Twin Falls, and western Snake River Plain regions, *in* Bonnichsen, B., et al., eds., Tectonic and Magmatic Evolution of the Snake River Plain Volcanic Province: Idaho Geological Survey Bulletin 30, p. 233–312.

Bonnichsen, B., and Kauffman, D.F., 1987, Physical features of rhyolite lava flows in the Snake River Plain volcanic province, southwestern Idaho, *in* Fink, J.H., eds., The Emplacement of Silicic Domes and Lava Flows: Geological Society of America Special Paper 212, p. 119–145, doi:10.1130/SPE212-p119.

Bonnichsen, B., Christiansen, R.L., Morgan, L.A., Moye, F.J., Hackett, W.R., Leeman, W.P., Honjo, N., Jenks, M.D., and Godchaux, M.M., 1989, Excursion 4A: Silicic volcanic rocks in the Snake River Plain–Yellowstone Plateau province, *in* Chapin, C.E., and Zidek, J., eds., Field Excursions to Volcanic Terranes in the Western United States: Volume II. Cascades and Intermountain West: New Mexico Bureau of Mines and Mineral Resources Memoir 47, p. 135–182.

Bonnichsen, B., Leeman, W., Honjo, N., McIntosh, W., and Godchaux, M., 2008, Miocene silicic volcanism in southwestern Idaho: Geochronology, geochemistry, and evolution of the central Snake River Plain: Bulletin of Volcanology, v. 70, p. 315–342, doi:10.1007/s00445-007-0141-6.

Boroughs, S., Wolff, J., Bonnichsen, B., Godchaux, M., and Larson, P., 2005, Large-volume, low-$\delta^{18}O$ rhyolites of the central Snake River Plain, Idaho, USA: Geology, v. 33, p. 821–824, doi:10.1130/G21723.1.

Boroughs, S., Wolff, J.A., Bonnichsen, B., Ellis, B.S., and Larson, P., 2012, Evaluating models of the origin of Miocene low-$\delta^{18}O$ rhyolites of the Yellowstone/Columbia River large igneous province: Earth and Planetary Science Letters, v. 313, p. 45–55, doi:10.1016/j.epsl.2011.10.039.

Branney, M.J., 1991, Eruption and depositional facies of the Whorneyside Tuff Formation, English Lake District: An exceptionally large-magnitude phreatoplinian eruption: Geological Society of America Bulletin, v. 103, no. 7, p. 886–897, doi:10.1130/0016-7606(1991)103<0886:EADFOT>2.3.CO;2.

Branney, M.J., and Kokelaar, B.P., 1992, A reappraisal of ignimbrite emplacement: changes from particulate to non-particulate flow during progressive aggradation of high-grade ignimbrite: Bulletin of Volcanology, v. 54, p. 504–520.

Branney, M.J., and Kokelaar, P., 1994, Volcanotectonic faulting, soft-state deformation, and rheomorphism of tuffs during development of a piecemeal caldera, English Lake District: Geological Society of America Bulletin, v. 106, p. 507–530, doi:10.1130/0016-7606(1994)106<0507:VFSSDA>2.3.CO;2.

Branney, M.J., and Kokelaar, B.P., 2002, Pyroclastic Density Currents and the Sedimentation of Ignimbrites: Geological Society of London Memoir 27, 143 p.

Branney, M.J., Barry, T.L., and Godchaux, M.M., 2004, Sheath folds in rheomorphic ignimbrites: Bulletin of Volcanology, v. 66, p. 485–491, doi:10.1007/s00445-003-0332-8.

Branney, M., Bonnichsen, B., Andrews, G., Ellis, B., Barry, T., and McCurry, M., 2008, Snake River (SR)–type volcanism at the Yellowstone hotspot track: Distinctive products from unusual, high-temperature silicic supereruptions: Bulletin of Volcanology, v. 70, p. 293–314, doi:10.1007/s00445-007-0140-7.

Brown, R.J., Branney, M.J., Maher, C., and Dávila-Harris, P., 2010, Origin of accretionary lapilli within ground-hugging density currents: Evidence from pyroclastic couplets on Tenerife: Geological Society of America Bulletin, v. 122, no. 1–2, p. 305–320, doi:10.1130/B26449.1.

Brown, R.J., Bonadonna, C., and Durant, A.J., 2012, A review of volcanic ash aggregation: Physics and Chemistry of the Earth, Parts A/B/C, v. 45, p. 65–78. doi:10.1016/j.pce.2011.11.001.

Carrasco-Núñez, G., and Branney, M.J., 2005, Progressive assembly of a massive layer of ignimbrite with normal-to-reverse compositional zoning: The Zaragoza ignimbrite of central Mexico: Bulletin of Volcanology, v. 68, p. 3–20, doi:10.1007/s00445-005-0416-8.

Cathey, H.E., and Nash, B.P., 2004, The Cougar Point Tuff: Implications for thermochemical zonation and longevity of high-temperature, large-volume silicic magmas of the Miocene Yellowstone hotspot: Journal of Petrology, v. 45, p. 27–58, doi:10.1093/petrology/egg081.

Cathey, H.E., and Nash, B.P., 2009, Pyroxene thermometry of rhyolite lavas of the Bruneau–Jarbidge eruptive center, central Snake River Plain: Journal of Volcanology

and Geothermal Research, v. 188, no. 1–3, p. 173–185, doi:10.1016/j.jvolgeores.2009.05.024.

Champion, D.E., Lanphere, M.A., Anderson, S.R., and Kuntz, M.A., 2002, Accumulation and subsidence of late Pleistocene basaltic lava flows of the eastern Snake River Plain, Idaho, *in* Link, P.K., and Mink, L.L., eds., Geology, Hydrology, and Environmental Remediation: Idaho National Engineering and Environmental Laboratory, Eastern Snake River Plain, Idaho: Geological Society of America Special Paper 353, p. 175–192.

Christiansen, R.L., 2001, The Quaternary and Pliocene Yellowstone Plateau Volcanic Field of Wyoming, Idaho, and Montana: U.S. Geological Survey Professional Paper 729-G, 146 p.

Christiansen, R.L., Foulger, G.R., and Evans, J.R., 2002, Upper-mantle origin of the Yellowstone hotspot: Geological Society of America Bulletin, v. 114, p. 1245–1256, doi:10.1130/0016-7606(2002)114<1245:UMOOTY>2.0.CO;2.

Doherty, D.J., McBroome, L.A., and Kuntz, M., 1979, Preliminary geological interpretation and lithologic log of the exploratory geothermal test well (INEL-1), Idaho National Engineering Laboratory, Eastern Snake River Plain, Idaho: U.S. Geological Survey Open-File Report 79-1248, 10 p.

Drew, D.L., Bindeman, I.N., Watts, K.E., Schmitt, A.K., Fu, B., and McCurry, M., 2013, Crustal-scale recycling in caldera complexes and rift zones along the Yellowstone hotspot track: O and Hf isotopic evidence in diverse zircons from voluminous rhyolites of the Picabo volcanic field, Idaho: Earth and Planetary Science Letters, v. 381, p. 62–77, doi:10.1016/j.epsl.2013.08.007.

Ellis, B., and Branney, M.J., 2010, Silicic phreatomagmatism in the Snake River Plain: The Deadeye Member: Bulletin of Volcanology, v. 72, p. 1241–1257, doi:10.1007/s00445-010-0400-9.

Ellis, B., Barry, T., Branney, M.J., Wolff, J.A., Bindeman, I., Wilson, R., and Bonnichsen, B., 2010, Petrologic constraints on the development of a large-volume, high-temperature, silicic magma system: The Twin Falls eruptive centre, central Snake River Plain: Lithos, v. 120, p. 475–489, doi:10.1016/j.lithos.2010.09.008.

Ellis, B., Branney, M.J., Barry, T.L., Barfod, D., Bindeman, I., Wolff, J.A., and Bonnichsen, B., 2012, Geochemical correlation of three large-volume ignimbrites from the Yellowstone hotspot track, Idaho, USA: Bulletin of Volcanology, v. 74, p. 261–277, doi:10.1007/s00445-011-0510-z.

Ellis, B.S., Wolff, J.A., Boroughs, S., Mark, D.F., Starkel, W.A., and Bonnichsen, B., 2013, Rhyolitic volcanism of the central Snake River Plain: A review: Bulletin of Volcanology, v. 75, p. 745–764, doi:10.1007/s00445-013-0745-y.

Ellis, B.S., Bachmann, O., and Wolff, J.A., 2014, Cumulate fragments in silicic ignimbrites: The case of the Snake River Plain: Geology, v. 42, no. 5, p. 431–434, doi:10.1130/G35399.1.

Ferguson, C.A., McIntosh, W.C., and Miller, C.F., 2012, Silver Creek caldera—The tectonically dismembered source of the Peach Spring Tuff: Geology, v. 41, p. 3–6, doi:10.1130/G33551.1.

Finn, D.R., Coe, R.S., Kelly, H., Branney, M.J., Knott, T.R., Reichow, M.K., 2015, Magnetic anisotropy in rhyolitic ignimbrite, Snake River Plain: Implications for using remnant magnetism of volcanic rocks for correlation, paleomagnetic studies, and geological reconstructions: Journal of Geophysical Research, Solid Earth, v. 120, p. 4014–4033, doi:10.1002/2014JB011868.

Hackett, W.R., Moye, F.J., and Bonnichsen, B., 1989, Day 5: Silicic volcanism in the SRP-YP province, *in* Chapin, C. E., and Zidek, J., eds., Field Excursions to Volcanic Terranes in the Western United States: Volume II. Cascades and Intermountain West: New Mexico Bureau of Mines and Mineral Resources Memoir 47, p. 160–167.

Henry, C.D., and Wolff, J.A., 1992, Distinguishing strongly rheomorphic tuffs from extensive silicic lavas: Bulletin of Volcanology, v. 54, p. 171–186.

Hildreth, W., and Moorbath, S., 1988, Crustal contributions to arc magmatism in the Andes of central Chile: Contributions to Mineralogy and Petrology, v. 98, no. 4, p. 455–489, doi:10.1007/BF00372365.

James, D.E., Fouch, M.J., Carlson, R.W., and Roth, J.B., 2011, Slab fragmentation, edge flow and the origin of the Yellowstone hotspot track: Earth and Planetary Science Letters, v. 311, p. 124–135, doi:10.1016/j.epsl.2011.09.007.

Kneller, B.C., and Branney, M.J., 1995, Sustained high-density turbidity currents and the deposition of thick massive sands: Sedimentology, v. 42, no. 4, p. 607–616, doi:10.1111/j.1365-3091.1995.tb00395.x.

Knott, T.R., Reichow, M.K., Branney, M.J., Finn, D.R., Coe, R.S., Storey, M., and Bonnichsen, B., 2016, Rheomorphic ignimbrites of the Rogerson Formation, central Snake River Plain, USA: Record of mid-Miocene rhyolitic explosive eruptions and associated crustal subsidence along the Yellowstone hotspot-track: Bulletin of Volcanology (in press).

Konstantinou, A., Strickland, A., Miller, E.L., and Wooden, J.P., 2012, Multistage Cenozoic extension of the Albion–Raft River–Grouse Creek metamorphic core complex: Geochronologic and stratigraphic constraints: Geosphere, v. 8, no. 6, p. 1429–1466, doi:10.1130/GES00778.1.

Leeman, W.P., 1982, Development of the Snake River Plain–Yellowstone Plateau province, Idaho and Wyoming: An overview and petrologic model, *in* Bonnichsen, B., and Breckenridge, R.M., eds., Cenozoic Geology of Idaho: Idaho Bureau of Mines and Geology Bulletin 26, p. 155–177.

Leeman, W., Annen, C., and Dufek, J., 2008, Snake River Plain–Yellowstone silicic volcanism: Implications for magma genesis and magma fluxes, *in* Annen, C., and Zellmer, G.F., eds., Dynamics of Crustal Magma Transfer, Storage and Differentiation: Geological Society of London Special Publication 304, p. 235–259.

Lipman, P.W., 1984, The roots of ash-flow calderas in North America: Windows into the tops of granitic batholiths: Journal of Geophysical Research, v. 89, p. 8801–8841, doi:10.1029/JB089iB10p08801.

Lowry, A.R., Ribe, N.M., and Smith, R.B., 2000, Dynamic elevation of the Cordillera, western United States: Journal of Geophysical Research–Solid Earth, v. 105, p. 23,371–23,390, doi:10.1029/2000JB900182.

Malde, H.E., and Powers, H.A., 1962, Upper Cenozoic stratigraphy of the western Snake River Plain, Idaho: Geological Society of America Bulletin, v. 73, no. 10, p. 1197–1210, doi:10.1130/0016-7606(1962)73[1197:UCSOWS]2.0.CO;2.

Marti, J., Diez-Gil, J.L., and Ortiz, R., 1991, Conduction model for the thermal influence of lithic clasts in mixtures of hot gases and ejecta: Journal of Geophysical Research, v. 96, p. 21,879–21,885, doi:10.1029/91JB02149.

Mason, B.G., Pyle, D.M., and Oppenheimer, C., 2004, The size and frequency of the largest explosive eruptions on Earth: Bulletin of Volcanology, v. 66, p. 735–748, doi:10.1007/s00445-004-0355-9.

McCurry, M., and Rodgers, D.W., 2009, Mass transfer along the Yellowstone hotspot track I: Petrologic constraints on the volume of mantle-derived magma: Journal of Volcanology and Geothermal Research, v. 188, p. 86–98, doi:10.1016/j.jvolgeores.2009.04.001.

McCurry, M., Watkins, A.M., Parker, J.L., Wright, K., and Hughes, S.S., 1996, Preliminary volcanological constraints for sources of high-grade, rheomorphic ignimbrites of the Cassia Mountains, Idaho: Implications for the evolution of the Twin Falls volcanic center: Northwest Geology, v. 26, p. 81–91.

McDonough, W.F., and Sun, S.S., 1995, The composition of the Earth: Chemical Geology, v. 120, no. 3, p. 223–253, doi:10.1016/0009-2541(94)00140-4.

McQuarrie, N., and Rodgers, D.W., 1998, Subsidence of a volcanic basin by flexure and lower crustal flow: The eastern Snake River Plain, Idaho: Tectonics, v. 17, no. 2, p. 203–220, doi:10.1029/97TC03762.

Miller, E.I., Dumitru, T.A., Brown, R.W., and Gans, P.B., 1999, Rapid Miocene slip on the Snake Range–Deep Creek Range fault system, east-central Nevada: Geological Society of America Bulletin, v. 111, p. 886–905, doi:10.1130/0016-7606(1999)111<0886:RMSOTS>2.3.CO;2.

Morgan, L.A., and McIntosh, W.C., 2005, Timing and development of Heise volcanic field, Snake River Plain, Idaho, western USA: Geological Society of America Bulletin, v. 117, p. 288–306, doi:10.1130/B25519.1.

Mytton, J.W., Williams, P.L., and Morgan, W.A., 1990, Geologic Map of the Striker 4 Quadrangle, Cassia County, Idaho: U.S. Geological Survey Miscellaneous Investigations Series Map I-2052, scale 1:48,000, 1 sheet.

Nash, B.P., Perkins, M.E., Christensen, J.N., Lee, D.C., and Halliday, A.N., 2006, The Yellowstone hotspot in space and time: Nd and Hf isotopes in silicic magmas: Earth and Planetary Science Letters, v. 247, p. 143–156, doi:10.1016/j.epsl.2006.04.030.

Oakley, W.L., and Link, P.K., 2006, Geologic Map of the Davis Mountain Quadrangle, Gooding and Camas Counties, Idaho: Idaho Geological Survey Geologic Map 49, scale 1:24,000, 1 sheet.

Ochs, F.A., and Lange, R.A., 1999, The density of hydrous magmatic liquids: Science, v. 283, p. 1314–1317, doi:10.1126/science.283.5406.1314.

Peng, X., and Humphreys, E.D., 1998, Crustal velocity structure across the eastern Snake River Plain and the Yellowstone swell: Journal of Geophysical Research, v. 103, p. 7171–7186, doi:10.1029/97JB03615.

Perkins, M.E., Nash, W.P., Brown, F.H., Fleck, R.J., 1995, Fallout tuffs of Trapper Creek Idaho—a record of Miocene explosive volcanism in the Snake River Plain volcanic province: Geological Society of America Bulletin, v. 107, p. 1484–1506.

Perkins, M.E., Williams, S.K., Brown, F.H., Nash, W.P., and McIntosh, W., 1998, Sequence, age, and source of silicic fallout tuffs in middle to late Miocene basins of the northern Basin and Range Province: Geological Society of America Bulletin, v. 110, p. 344–360, doi:10.1130/0016-7606(1998)110<0344:SAASOS>2.3.CO;2.

Pierce, K.L., and Morgan, L.A., 1992, The track of the Yellowstone hot spot: Volcanism, faulting, and uplift, *in* Link, P.K., Kuntz, M.A., and Platt, L.B., eds., Regional Geology of Eastern Idaho and Western Wyoming: Geological Society of America Memoir 179, p. 1–53, doi:10.1130/MEM179-p1.

Pyle, D.M., 2000, Sizes of volcanic eruptions, *in* Sigurdsson, H., et al., eds., Encyclopedia of Volcanoes: San Diego, California, Academic Press, p. 263–269.

Rivera, T. A., Storey, M., Zeeden, C., Hilgen, F. J., and Kuiper, K., 2011, A refined astronomically calibrated $^{40}Ar/^{39}Ar$ age for Fish Canyon sanidine: Earth and Planetary Science Letters, v. 311, p. 420–426.

Rodgers, D.W., Ore, H.T., Bobo, R.T., McQuarrie, N., and Zentner, N., 2002, Extension and subsidence of the eastern Snake River Plain, Idaho, *in* Bonnichsen, B., White, C.M., and McCurry, M., eds., Tectonic and Magmatic Evolution of the Snake River Volcanic Province: Idaho Geological Survey Bulletin 30, p. 121–155.

Rust, A.C., Cashman, K.V., and Wallace, P.J., 2004, Magma degassing buffered by vapor flow through brecciated conduit margins: Geology, v. 32, no. 4, p. 349–352, doi:10.1130/G20388.2.

Self, S., 2006, The effects and consequences of very large explosive volcanic eruptions: Philosophical Transactions of the Royal Society, ser. A, Mathematical, Physical and Engineering Sciences, v. 364, p. 2073–2097, doi:10.1098/rsta.2006.1814.

Shervais, J.W., Vetter, S.K., and Hanan, B.B., 2006, Layered mafic sill complex beneath the eastern Snake River Plain: Evidence from cyclic geochemical variations in basalt: Geology, v. 34, p. 365–368, doi:10.1130/G22226.1.

Shervais, J.W., Schmitt, D.R., Nielson, D., Evans, J.P., Christiansen, E.H., Morgan, L., Shanks, W.C.P., Prokopenko, A.A., Lachmar, T., Liberty, L.M., Blackwell, D.D., Glen, J.M., Champion, D., Potter, K.E., and Kessler, J.A., 2013, First results from HOTSPOT: The Snake River Plain Scientific Drilling Project, Idaho, U.S.A.: Scientific Drilling, v. 15, p. 36–45, doi:10.5194/sd-15-36-2013.

Smith, R.L., 1960, Zones and Zonal Variations in Welded Ash-Flows: U.S. Geological Survey Professional Paper 354-F, p. 149–158.

Smith, R.L., 1979, Ash-flow magmatism, *in* Chapin, C.E., and Elston, W.E., eds., Ash-Flow Tuffs: Geological

Society of America Special Paper 180, p. 5–28, doi:10.1130/SPE180-p5.

Sparks, R.S.J., Self, S., and Walker, G.P.L., 1973, Products of ignimbrite eruptions: Geology, v. 1, no. 3, p. 115–118, doi:10.1130/0091-7613(1973)1<115:POIE>2.0.CO;2.

Sparlin, M.A., Braile, L.W., and Smith, R.B., 1982, Crustal structure of the eastern Snake River Plain determined from ray trace modelling of seismic refraction data: Journal of Geophysical Research–Solid Earth, v. 87, p. 2619–2633, doi:10.1029/JB087iB04p02619.

Sumner, J.M., and Branney, M.J., 2002, Emplacement history of a remarkable heterogeneous chemically zoned, rheomorphic and locally lava-like ignimbrite: 'TL' on Gran Canaria: Journal of Volcanology and Geothermal Research, v. 115, p. 109–138, doi:10.1016/S0377-0273(01)00311-0.

Troll, V.R., Emeleus, C.H., and Donaldson, C.H., 2000, Caldera formation in the Rum Central igneous complex, Scotland: Bulletin of Volcanology, v. 62, p. 301–317, doi:10.1007/s004450000099.

Williams, P.L., Mytton, J.W., and Covington, H.R., 1990, Geologic Map of the Stricker 1 Quadrangle, Cassia, Twin Falls, and Jerome Counties, Idaho: U.S. Geological Survey Miscellaneous Investigations Series Map I-2078, 1:48,000, 1 sheet.

Williams, P.L., Covington, H.R., and Mytton, J.W., 1991, Geologic Map of the Stricker 2 Quadrangle, Twin Falls, and Cassia Counties, Idaho: U.S. Geological Survey Miscellaneous Investigations Series Map I-2078, 1:48,000, 1 sheet.

Williams, P.L., Mytton, J.W., and Morgan, W.A., 1999, Geologic Map of the Stricker 3 Quadrangle, Idaho and Nevada: U.S. Geological Survey Miscellaneous Investigations Series Map I-2633, 1:48,000, 1 sheet.

Wood, S.H., and Clemens, D.M., 2002, Geologic and tectonic history of the western Snake River Plain, Idaho and Oregon, *in* Bonnichsen, B., McCurry, M., and White, C.M., eds., Tectonic and Magmatic Evolution of the Snake River Plain Volcanic Province: Idaho Geological Survey Bulletin 30, p. 69–103.

Wright, K.E., McCurry, M., and Hughes, S.S., 2002, Petrology and geochemistry of the Miocene tuff of McMullen Creek, central Snake River Plain, *in* Bonnichsen, B., McCurry, M., and White, C.M., eds., Tectonic and Magmatic Evolution of the Snake River Plain Volcanic Province: Idaho Geological Survey Bulletin 30, p. 177–194.

Youngquist, W., and Haegele, J.R., 1956, Geological Reconnaissance of the Cassia Mountains Region, Twin Falls and Cassia Counties, Idaho: Idaho Bureau of Mines and Geology Pamphlet 110, 18 p.

Science Editor: Aaron J. Cavosie
Associate Editor: Nancy Riggs

Manuscript Received 24 March 2015
Revised Manuscript Received 24 December 2015
Manuscript Accepted 25 January 2016

Printed in the USA